



University of Glasgow | School of Engineering

Wireless Power Transfer in Wearable Smart Contact Lenses

Student: Mengyao Yuan

GUID:

1st Supervisor: Hadi Heidari

Abstract

In 2016, a smart contact lens was developed by Google company which aimed to directly implanting micro-smart lenses into the human eye to test blood sugar percentage by tears. However, small sizes implantable devices such as contact lens requires power transfer unit for continuously power supply. Thus, this project aims to design a power transfer unit with Inductively Coupled Power Transfer (ICPT) technology for smart contact lens which works under 2.45GHz to power an LED at load. The coil size is designed as 10mm inner diameter, 12mm outer diameter and 0.2mm wire width. Additionally, polydimethylsiloxane (PDMS) is used as the contact lens substrate. During the simulation, different eye models were built since the coil needs to be warped on top of lens and the eyeball, and under different conditions the S_{11} parameter is adjusted to around -10dB. The antenna is fabricated by technician in school, due to the technology restriction, the antenna was fabricated with unequal line width, which causes a resonate frequency shift to 900MHz with -8dB S_{11} value. To power an LED at load side, full-wave and half-wave rectifiers are built separately with different component values and send to fabrication. The antenna performance was tested under three conditions, in air, on human hand, and on water surface to imitate the liquid condition in human eye, but since the dielectric constant varies in each case, and for fabrication there is an extra circuit unit which effecting the copper coil numbers, the tested resonant frequency is not as desired values.

Acknowledgements

I am very grateful to the guidance and support from my first supervisor Dr. Hadi Heidari and the postdoctoral Dr. Rupam Das who always encourage me to think and move further. In addition to that, the operational advices and technical help from PhD students from meLab group is really precious, I could not finish the task effectively without their kindness assistance.

Contents

Abstract	2
Acknowledgements	3
1. Introduction	6
1.1 Wireless Power Transfer	6
1.2 Wireless Power Transfer Applications	7
2. Wireless Power Transfer	10
2.1 Ultrasonic Power Transfer	10
2.2 Capacitively Coupled Power Transfer	11
2.3 Inductively Coupled Power Transfer	12
2.3.1 ICPT Basic Principles	13
2.3.2 ICPT Coil Design Principles	13
2.3.3 ICPT Coil Design Parameters	14
2.4 FDA Verified Medical Frequency Bands	16
2.5 Circuitry	17
2.5.1 Half-Wave Bridge Rectifier	17
2.5.2 Full-Wave Bridge Rectifier	17
2.6 Encapsulation	18
3. Design	20
3.1 Antenna Design	20
3.1.1 Leading Factor of Antenna Design	20
3.1.2 Design Method	21
3.1.3 Receiver Antenna Design in HFSS	22
3.1.4 Transmitter Antenna Design in HFSS	29
3.2 Circuit design	29
3.3 PCB design	32
4. Result	33
4.1 Fabricated Antenna	33
4.2 Laser Cutting	36
5. Analysis and Discussion	37
5.1 Geometry Effect on Antenna	37
5.2 Different Conditions Effect on Antenna	38
6. Conclusions and Further Work	39
6.1 Conclusions	39
6.2 Suggestions for Further Work	39
6.2.1 Antenna Improvement	39
6.2.2 Fabrication Improvement	40
Reference	41

List of Figure

Figure 1. WPT applications.	8
Figure 2. Basic UPT system applied on human body	10
Figure 3. Basic UPT system applied on human body	11
Figure 4. Basic ICPT system construction	13
Figure 5. ICPT coil modelling design process	13
Figure 6. Half-wave rectifier	17
Figure 7. Full-wave bridge rectifier.....	18
Figure 8. Circular Spiral Antenna	21
Figure 9. Eye model with dimension.....	22
Figure 10. Flat geometry with simulation results.....	23
Figure 11. Bending geometry with simulation results.....	24
Figure 12. PDMS layer and warping attempts	25
Figure 13. Projected antenna outcome	26
Figure 14. Current density of coil.....	26
Figure 15. S11 simulation result of contact lens antenna.....	27
Figure 16. Smith Chart of contact lens antenna.....	28
Figure 17. Transmitter antenna geometry.....	29
Figure 18. Full-wave rectifier.....	30
Figure 19. Full wave rectifier circuit construction	30
Figure 20. Output voltage vs Input voltage of testing circuit.....	31
Figure 21. Half-wave rectifier.	31
Figure 22. Half-wave rectifier circuit construction	32
Figure 23. Two versions of PCB design with different component size and position.	32
Figure 24. Fabricated antenna compared with a five pence size.....	33
Figure 25. Antenna test under different conditions	34
Figure 26. S11 parameter under different condition.	35
Figure 27. PCB compared with drawing graph.	36
Figure 28. Laser cutting on different materials	36
Figure 29. Antenna design geometry related to electrical parameters.	37
Figure 30. Circuit in PCB.	37
Figure 31. Second-version antenna.	39
Figure 32. Serpentine antenna.	40

List of Table

Table 1. Medical Frequency Band.....	16
Table 2. Electromagnetic parameters of eye tissues	23

1. Introduction

In biomedical field, characteristics of an organism are collected by biomedical chips through functional transformation and displayed back in electronic devices. In the development of biomedical chips, integration and miniaturization are the main concerns in future design. Since such characteristics of miniaturization and integration can enable biomedicine to achieve the greatest precision of measurement, and even bring such accuracy to the level of molecules and atoms, in other words, the development of biomedicine would step onto an unprecedented prosperous development stage. However, implantable electronic devices are still disturbing, in the medical field, implantable electronic devices have existed for a long time. For example, pacemakers can be implanted in the human body to save the lives of patients at critical moments. Implantable electronic devices have great potential in the medical field, and one of the key issues is how to charge devices. The current solution, one is to use a battery that lasts for a long time, which will cause the device to be bulky, and when it is exhausted, it still needs to be surgically removed, the following paragraph introduce the existing technology of wireless power transfer.

1.1 Wireless Power Transfer

Wireless Power Transfer (WPT) technology first comes to commercial field from 2010, and then one year later, a number of Japanese manufacturers took the lead in displaying their commercial devices related to wireless charging technology. Compactly, in the second half of 2011, some consumer electronics manufacturers began to apply wireless charging technology to smart phones and other portable devices, which was gradually introduced to the public. Future wireless charging technologies will allow all mobile devices to be embedded with built-in receivers and transmitters that are deployed everywhere in public areas such as cafes, hotels, airports or fast food restaurants, etc. Although commercial electronics is an obvious target market, medical and industrial portable devices are also segments that could benefit from wireless power, enabling waterproof enclosures and reducing the number of charging ports that are often used and can cause unnecessary breakdowns due to repeated insertion of charging cables.

The reason why WPT technology is so popular and futuristic is because of its portability and safety. Since for WPT system, there is no power contact design which can avoid the danger of electric shock, and without any exposed power transmission components, there

will be less air moisture, oxygen and other erosion, furthermore, there is no contact, so there will be no mechanical wear and tear in the connection and separation. As for medical implantable devices, the embedded devices can be charged without damaging the body's tissues, eliminating the risk of infection without wires running through the skin and other autologous tissues. Since there is no need to connect a wire when charging, devices are just be put near the charger instead, thus technically, a single charger can supply power to multiple electrical devices, which can save the trouble of multiple chargers, countless power sockets and endless wires winding each other when there are redundant electrical devices. There is no doubt that WPT will affect the power transferring efficiency that energy storage efficiency will be less than real contact devices, and due to their low charging efficiency, the charging speed would be relatively slow at the same input power as well. However, more power transfer and management unit, such as extra electronic circuits and coils on both transmitting sides, are required for a WPT system which makes the cost of the device higher than normal power charging facilities. The compatibility of WPT devices are becoming challenging as well since wireless charging devices of different brands cannot be exchanged since there is no uniform standard. In recent years, Wireless Power Consortium has been pushing for standardisation, with the promise of uniform standards.

1.2 Wireless Power Transfer Applications

WPT is widely used upon implantable and wearable devices nowadays, such as pacemaker, cochlear implants and contact lens. Those devices are generally implanted into human body to detect physical functions, either through stimulating electronic signals or enlarging signals by packaged sensors.

For example, a pacemaker, shown in Figure 1 (a)[1], is an electronic treatment instrument implanted in the body, which sends out electric pulses of energy provided by batteries through the pulse generator. It stimulates the myocardium contacted by the electrode through the conduction of the wire electrode, making the heart excited and contracted, so as to achieve the purpose of treating the cardiac dysfunction caused by some arrhythmias. In addition to the special type pacemaker, single chamber pacemaker battery life is commonly eight years or more, double chamber pacemaker battery life can be less than six years, and three chamber pacemaker deceases to four years. Which means at least every eight years, implanted pacemaker needs to be checked or replaced by surgery which does harm to human body and may cause second damages[2].

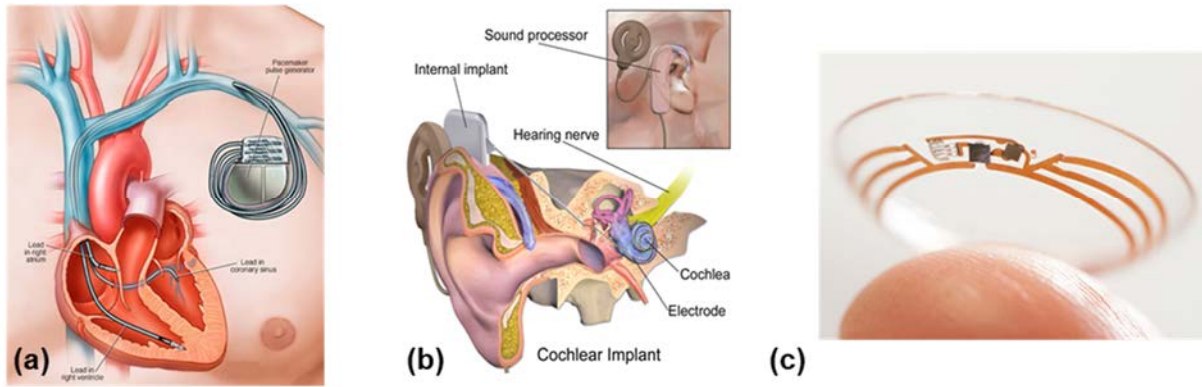


Figure 1. WPT applications on (a) pacemaker (b) cochlear implants and (c) smart contact lens.

As for cochlear implants shown in Figure 1(b) [3], sound signal is converted into a certain coded form of electrical signals by external speech processor, and the auditory nerve is directly stimulated through the implanted electrode system to restore or reconstruct the hearing function of deaf people. With the development of technology, cochlear implants are now routinely used worldwide to treat severe to total deafness. Although the cost of cochlear implant has been approximately £50,000 per person, due to the high demands of fighting with deafness, it is the only implant whose technology upon power transfer unit has been mature enough to ensure the device lifetime to be 70 to 80 years.

For smart contact lens as Figure 1 (c) [4] shows, Google has been involved in this field since 2014. Google's Life Sciences affiliate Verily Life Sciences and Alcon, the eye division of Swiss pharmaceutical giant Novartis, announced they are teaming up to develop a smart contact lens for diabetics. But as recently as November 2016, Novartis announced it was abandoning its goal of clinical trials of its products. However, biomedical engineers are already using smart contact lens to diagnose diseases in laboratories around the world, and thanks to the development of flexible tiny translucent circuits and the possibility of hydrogel lenses, these smart contact lenses have made great progress and are moving into commercial field. Finally, the "Triggerfish smart contact lens" was made by Sensimed, a biotechnology company based in Lausanne, Switzerland. This smart contact lens was measured about 14mm in diameter and only 100 to 200 microns thick, and it has a small curved surface to accommodate sensors and microelectronic circuits for monitoring, energy management and data transfer. Moreover, this soft disposable contact lens uses a piezo resistive strain sensor to measure intraocular pressure. The sensor is stretched by fluid pressure to detect subtle changes around the cornea [5].

However, for limited space on contact lens, it is not possible to carry batteries with those small devices, they also require WPT system to supply continuously charging power to them. In conclusion, implantable and wearable devices such as pacemakers, cochlear implants and smart contact lens, due to their implanting characteristic, WPT plays an important role in the power transfer and management unit, which will be benefit for all implantable and wearable biomedical devices when the stability and safety are verified.

2. Wireless Power Transfer

WPT is a technology that transfers electrical energy from a power generating device or a power supply terminal to a power receiving device without passing through any electrical conductor. Thus, it is also a generic term that can be achieved using a variety of different techniques, including electric, magnetic, and electromagnetic waves. Conceptually, the transmitter side converts the electrical energy into a corresponding field energy state, which is transmitted through a space and received by one or more receivers and converted back into electrical energy. WPT technology nowadays is divided into two main categories: non-radiative and radiative power transfer. Non-radiative techniques are mainly based on inductively coupled power transfer between the coils, where energy is transmitted through the magnetic field. Examples of no-radiative power transfer applications include electric toothbrush charging, radio frequency identification, smart cards, heart rate regulators, and electric vehicle chargers. The focus of development now is on wireless charging technologies such as mobile phones. Radiative power transfer technology transmits energy by directional energy beams such as microwaves and lasers. This technology can transmit power under longer distance, but the transmitting side must be aimed at the receiving side to transmit power upon exact positions. However, WPT using radiative technology is still in the experimental stage, and the proposed use may be applied on solar power satellites and unmanned aerial vehicles. For implantable devices, the challenge would be reflected in device size and transfer efficiency. Therefore, the mostly competitive method of WPT system upon implantable devices are Ultrasonic Power Transfer (UPT), Capacitively Coupled Power Transfer (CCPT), and Inductively Coupled Power Transfer (ICPT)[6].

2.1 Ultrasonic Power Transfer

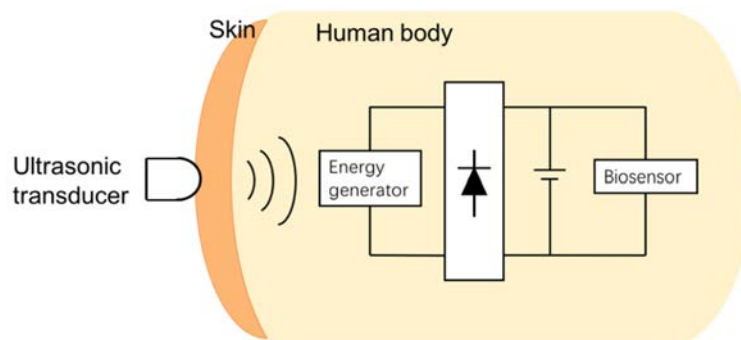


Figure 2.Basic UPT system applied on human body

As is shown in Figure 2, the main scheme of the UPT system design is that the ultrasonic generator generates and emits an ultrasonic signal from the external ultrasonic transducer, and the power module of the device implanted in the human body receives the ultrasonic signal, and then simultaneously converts it into an electrical signal of a certain voltage, which stores the electric energy in the power module, so as to realize energy supplement of the implantable cardiac pacemaker power. In addition to that, power consumption and charging process of rechargeable battery can be detected through external program-controlled apparatus under radio frequency communication. The ultrasonic generator is composed of a generator body and an associated ultrasonic transmitting probe for generating and transmitting an ultrasonic signal that transmits energy to the implanted device through the human skin.

Although using ultrasonic signal as the carrier of energy transmission can non-invasively penetrate human skin and muscle tissue, which prevents electromagnetic interference to the normal work of implanted devices such as electromagnetic inductively wireless charging technology, the power that UPT system can harvest so far is relatively low compared to other two methods, which is a debatable challenge it needs to be solved[7].

2.2 Capacitively Coupled Power Transfer

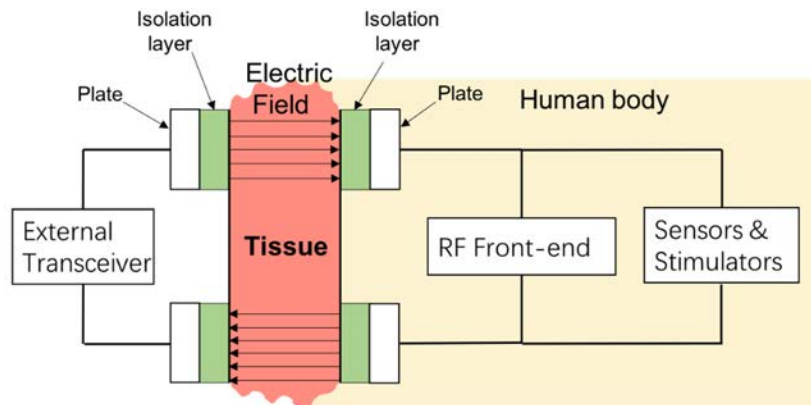


Figure 3.Basic UPT system applied on human body

The CCPT as Figure 3 shows, contains four parts, where one side capacitive plates and circuits are inside the human body and another side of capacitive plates and an external transceiver are outside the body. Electric field coupling or electrostatic coupling mode was generated in between the capacitive plates by distributed capacitance to transfer power. The coupling capacitor makes the two systems of strong current and weak current coupled and isolated through the capacitor, providing high frequency signal path, preventing the power

frequency current from entering the weak current system, and ensuring personal safety. With the coupling capacitor voltage sampling device, besides the above functions, it can also extract power frequency voltage for further protection and reclosing, playing the role of voltage transformer. On the external side, the capacitor is connected to an AC circuit, and the voltage of the circuit connected by a pin gradually increases, gradually accumulating charge in the electrode plate. When the voltage of the circuit connected by the pin drops, the charge accumulated when the potential is high and will be returned to the circuit, so is the other side. The capacitor is insulated by adding an isolation layer, and no current passes through the entire capacitor. As a coupling capacitor, its function is to allow AC signals to pass through normally, and to cut off the DC current of the upper amplifier circuit, so that it will not have an impact on the working point of the next amplifier circuit. There is no direct current path between the two plates of capacitor, so direct current cannot flow through. The two electrode plates of the capacitor can store charge, where it charges the capacitor with positive half cycle of alternating current, discharges the capacitor with negative half cycle, the charge and discharge continuously are equivalent to current flowing through the capacitor. However, the major disadvantage of this method is that the plates may increase the tissue temperature, causing patient discomfort. In addition, the human body is a non- magnetic material, during the process, the negligible magnetic field losses indicate that human tissue is absorbing the electric field as well. Except for that, the two capacitive plates should be bonded tightly with tissue which may cause problems for longer range and body moving conditions, however, CCPT system occupies more spaces and requires double components that leads to burdens for implantable system[8].

2.3 Inductively Coupled Power Transfer

The wireless charger principle relies on Faraday induction theory, which creates a magnetic field when current passes through the coil. The resulting magnetic field creates a voltage, which leads to a current, and then charges the battery. This is how wireless chargers get rid of the wires. At present, the most common wireless charging solutions are mainly electromagnetic induction, which induces a current through primary and secondary coils, thus transferring energy from the transmission segment to the receiving end.

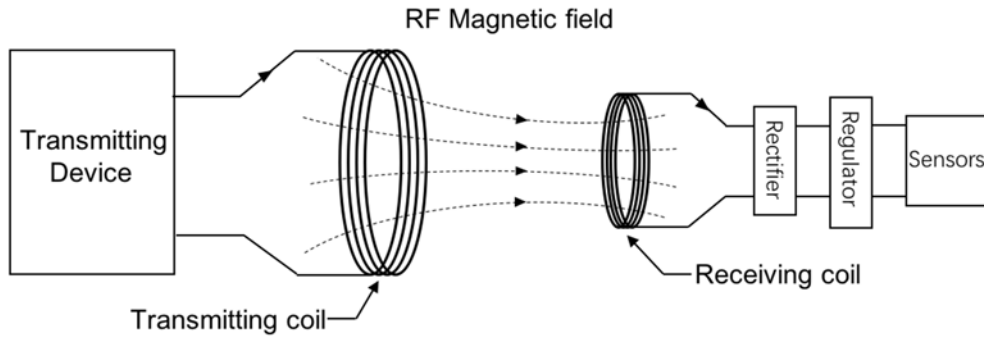


Figure 4. Basic ICPT system construction

Due to its scalability between low and high-power devices and the good efficiency performance under high potential system, ICPT technology becomes not only the oldest but also the most established for biomedical WPT.

2.3.1 ICPT Basic Principles

Different from CCPT, ICPT transfer power in between magnetic field instead electric field. According to Electromagnetic induction law, the magnetic flux changes in magnetic field will induce electromotive force in electric field. Thus, power can be transferred in magnetic field in between the transmitting and receiving coils. In Figure 4, a basic ICPT system construction is shown that power is transmitted from the transmitting devices as AC signal, and through the RF magnetic field, it is received by the receiving coil and then transferred to the load circuit. It is interesting to note that, ICPT system works under an AC waveform, so the receiver side usually requires an AC/DC converter to change the voltage and current from AC form to continuously stabilized DC ones, an AC/DC converter contains a rectifier and a regulator to enhance the stability of the DC signal.

2.3.2 ICPT Coil Design Principles

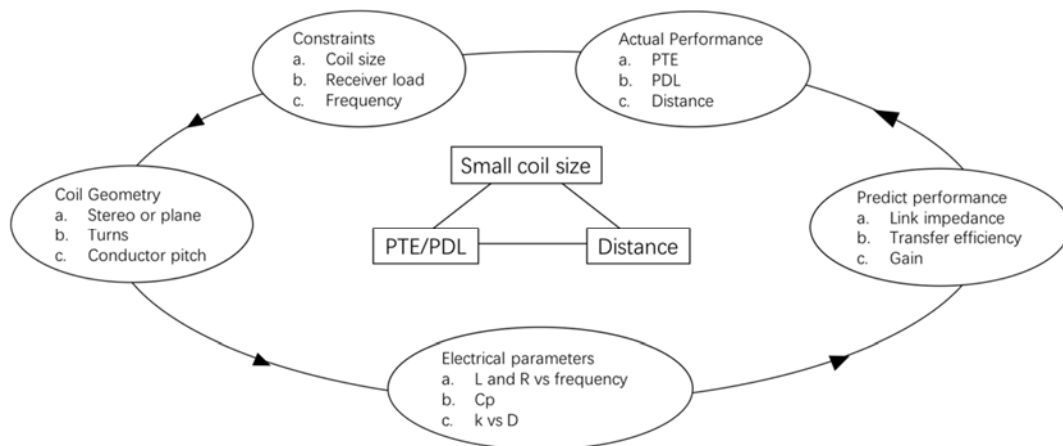


Figure 5. ICPT coil modelling design process

The equivalent circuit of whole system is shown in Figure 5. The first step of the design is always to list the design constraints based on the limitation of coil size, defining the receiver load and the resonating frequency. Next, fill as many turns as possible for better quality factor. Then determine whether the coil's self-resonant frequency is higher than the operating frequency. Usually for implantable and wearable devices, the quality factor is best around about -15dB, which is the most important step which ensures that the coil will still behave as an inductor when operating at that frequency. To improve the behavior of the coil, fewer turns and more separation between wires which affects the conductivity of the coil will change the resonate frequency. When designing the primary coil there are generally no limitations since the transmitter side is placed the outside body and its shape could vary with the carrier. However, when the coil geometries are changed, the electrical parameters of the coil which is linked with the alternation could be extracted to predict the performance by the power transfer efficiency (PTE) and power delivered to load (PDL). After comparing of the predicted performance with the targeting expectations, the geometry could be altered again to reach the best expected performance. Nevertheless, there is always compromising between small coil size, PTE/PDL and the transferring distance tolerance.

2.3.3 ICPT Coil Design Parameters

Based on the electromagnetic theory of a circular coil the function of magnetic field strength and the distance separation between two coils can be determined as follows in Eq.1[9]:

$$H(x, r) = \frac{I_r^2}{2\sqrt{(r^2+x^2)}} \quad (1)$$

where r is the coil radius, x is the separation between two coil and I_r is the magnitude of current. When the distance x is increased, a weaker magnetic field will be induced by another coil. After both coils have an acceptable quality factor a tuning capacitor should be connected to both coils which will make both the primary and implantable coils resonate at the same frequency. The resonant frequency of the LC tank circuit can be determined as Eq. 2[10] :

$$f = \frac{1}{2\pi\sqrt{LC_{total}}} \quad (2)$$

where L is the inductance of the coil, C is the total capacitance of the whole circuit. The inductance of the coil can be accurately determined by the LCR meter, but the total capacitance is relatively difficult to measure. C_{total} of the circuit is the sum of the coil's parasitic capacitance and the tuning capacitance. If the value of tuning capacitance is much

higher than the parasitic capacitance, the effect of parasitic capacitance can be ignored. Nevertheless, if the coil has tuned perfectly, it does not require an extra capacitor to shift the resonate frequency. However, if the inductor has inductance within one hundred micro henneries and is being tuned to resonate at a few megahertz, the parasitic capacitance will usually cause a resonant frequency shift and thus reduce the transmission efficiency at the desired operating frequency. Accurately determining the coil parasitic capacitance is important for boosting the transmission efficiency.

The aim of ICPT is to implement the highest power transfer efficiency under small sizes, this process can be achieved by adjusting the coil link parameters such as coupling coefficient k , mutual inductance M , and quality factor Q . For two coils with mutual inductance, their mutual inductance coefficient is the same, that is, the mutual inductance M is only related to the geometric size, the number of turns, the mutual position and the permeability of the media at the position of the coil. The tightness of the magnetic circuit coupling of the two mutual inductors is expressed by the coupling coefficient k , denoted by Eq. 3[10]:

$$k = \frac{M}{\sqrt{L_1 L_2}} \quad (3)$$

where M is the mutual inductance of the two-coil system with inductance of L_1 and L_2 . When $k=1$, it is fully coupled, that is, the magnetic field of the coil current not only passes through itself, but also passes through the mutual inductors. When the leakage flux is increased, the coupling performance is worse and the k value will be smaller. For electrical equipment that works on the principle of mutual inductance, it is best for coupling to be as close to 1. During the resonating process, there will be power loss, and this power loss position can be defined by quality factor, also called the quality factor of the inductor, which is the main parameter to measure the inductor device and is denoted as Eq. 4 for two-coil ICPT[10]:

$$Q = \frac{\omega L_{eff}}{ESR} = \frac{2\pi L_{self}(1-f^2/f_{self}^2)}{R_{dc}(1+f^2/f_h^2)} \quad (4)$$

where, L_{eff} and L_{self} is the effective inductance and self-resonant inductance of the coil, f and f_{self} is the operating and self-resonant frequency respectively, f_h denotes the frequency when AC power is doubled as DC power by [8] and R_{dc} is the DC resistance of the system. The higher the Q value of inductor, the smaller the loss. The theoretical efficiency is defined by the coupling coefficient and quality factor of both sides as Eq. 5 [11]:

$$\eta_{link} = \frac{k^2 Q_1 Q_2}{(1 + \sqrt{1 + k^2 Q_1 Q_2})^2} \quad (5)$$

As the equations indicated, the efficiency of the ICPT system relates to the product of k and Q , which is hard to achieve since these two parameters are defined contradicted with each other.

2.4 FDA Verified Medical Frequency Bands

For implantable and wearable devices, the applied frequency is a vital issue in the beginning of design. However, there are FDA verified medical frequency bands that can be used for implantable devices, which are listed from 13.56MHz to 2.45GHz as Table 1:

Table 1. Medical Frequency Band

<i>Fre. range (Centre Fre.) [MHz]</i>	<i>Type</i>	<i>Availability</i>	<i>Licensed users</i>
13.553 - 13.567 (13.56)	B	Worldwide	Fixed & Mobile services except Aeronautical mobile (R) service
26.957 - 27.283 (27.12)	B	Worldwide	Fixed & Mobile services except Aeronautical mobile service, CB Radio
40.66 - 40.7 (40.68)	B	Worldwide	Fixed, Mobile services & Earth exploration-satellite service
433.05 - 434.79 (433.92)	A	Only in Region 1, subject to local acceptance	Amateur service & radiolocation service, additional apply the provisions of footnote 5.280.
902 - 928 (915)	B	Region 2 only (with some exceptions)	Fixed, Mobile except aeronautical mobile & radiolocation service; in Region 2 additional Amateur service
2400 - 2500 (2450)	B	Worldwide	Amateur, amateur satellite, radiolocation & earth exploration-satellite service

As Table 1 shows, frequencies that listed from 13.56MHz to 2.45GHz in the table are verified applicable by FDA. Frequency bands such as 13.56MHz, 915MHz, and 2.45GHz are frequently used by implantable and wearable devices. However, there are two different types of frequency band, Type A and Type B, where Type A indicates that it must reach an agreement with other administrative authorities whose radiocommunication services may be affected during those frequency bands, and in applying this provision, the administration should take the latest relevant recommendations of ITU-R into consideration. However, radiocommunication services operating under Type B frequency bands must accept the harmful interference that may be caused by these applications. It is interesting to note that all the other frequency band is applicable worldwide except 433.92MHz and 915MHz, where Region 1 comprises Europe, Africa, the former Soviet Union, Mongolia, and the Middle East west of the Persian Gulf, including Iraq, Region 2 covers the Americas including Greenland, and some of the eastern Pacific Islands [12].

2.5 Circuitry

In terms of the coil resonating geometry, electromagnetic field is generated in between, but for normal LED or sensor circuits, direct current is mostly allowed to pass through, thus, to power a LED or normal sensor circuit, an AC/DC converter is needed. AC/DC converter is a device that converts alternating current into direct current, and its power flow can be two-way. The power flow from the power source to the load is called rectification, and the power flow from the load back to the power source is called active AC/DC converter. relatively large filtering capacitors are essential since it must be rectified and filtered, and the AC input side is usually added with EMC filtering and use of safety standard components, which limits the miniaturization of AC/DC power supply. Technically, there are two ways of rectifier, either full-wave bridge rectifier or half-wave rectifier, which relates to the numbers of diodes.

2.5.1 Half-Wave Bridge Rectifier

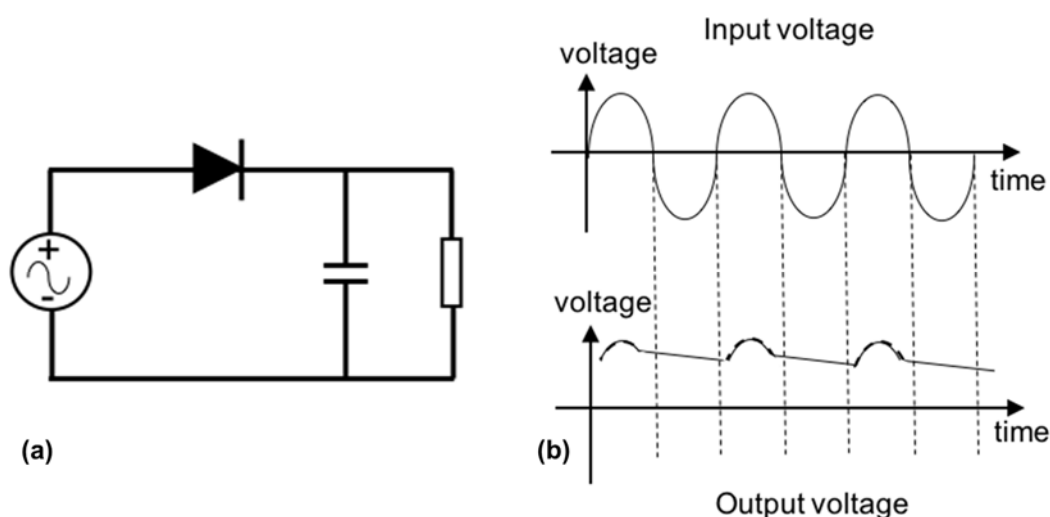


Figure 6. Half-wave rectifier (a) circuit (b) expecting output

Half-wave rectifier uses the unidirectional conductivity of the diode, which means when the input is the standard sine wave, the positive half of the sine wave is obtained and the negative half is lost. The smoothing capacitor there is for restore energy, which charges during the rising part of sine wave, and discharges when signal is negative, in order to change the AC signal to be more stable and plain as DC signal.

2.5.2 Full-Wave Bridge Rectifier

Bridge rectifier is an improvement of diode half-wave rectifier, where the half wave rectifier uses the single guide pass characteristic of diode to obtain the positive half of the sinusoidal

wave and lose the negative half when the input is the standard sine wave. However, bridge rectifier utilizes four diodes that are paired to ensure when the positive half of the sine wave is input, two tubes are conducting, and a positive output is gotten; when the negative half of the sine wave is input, the other two diodes are connected as well, but with reversed direction, thus positive half of the sine wave can also be achieved. The efficiency of bridge rectifier for input sinusoidal wave is twice that of half wave rectifier, however, bridge rectifier is the first step in converting alternating current to direct current.

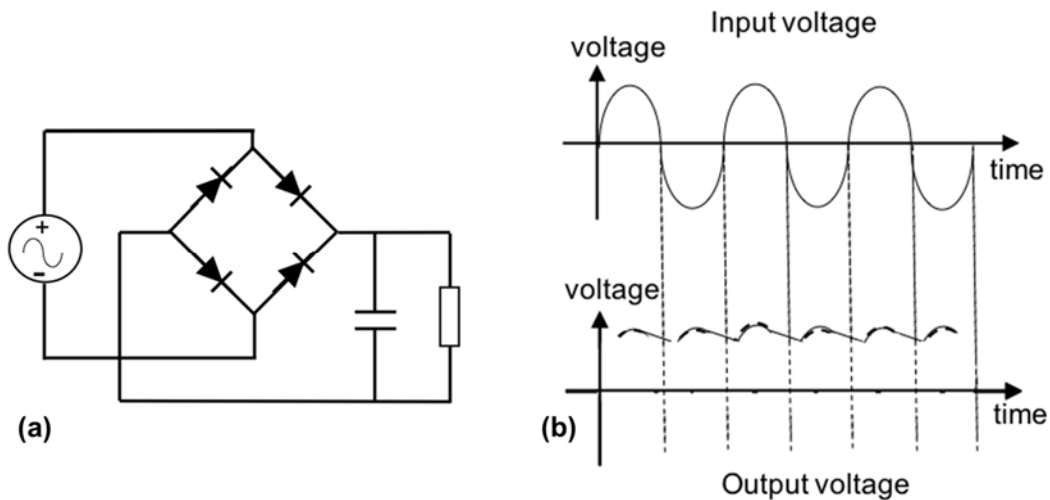


Figure 7. Full-wave bridge rectifier (a) circuit (b) expecting output

2.6 Encapsulation

For smart contact lens, except the power transferring coil size, the encapsulation is also a vital issue since contact lens are usually soft and stretchable to be comfortable on human eyes. Thus, for this project, PDMS is used for the encapsulation of the smart contact lens. PDMS as a kind of polymer material, is not only cheap and easy to process, but it can also copy microstructure by special pouring method, additionally, it is easy to pass through visible light and partial ultraviolet, and is biological compatible, which is a kind of material that is widely used in the preparation of microfluidic chips at present. However, the single microfluidic chip made by PDMS is not suitable for applications that requires high mechanical rigidity since it is soft in texture. But the mixed packaging of PDMS, silicon and glass can be designed to foster strengths and circumvent weaknesses, which also gives full play to the advantages of various materials, and the use to meet different requirements. Since cured PDMS surface has limited adhesive force, a pair of molded PDMS substrates without any treatment can be naturally bonded by virtue of the gravity between molecules, but with weak adhesive strength, which is prone to leakage. At present, there are various

methods of bonding PDMS with silicon-based materials at low temperature. One way is to make Silicon-PDMS multi-layer structure micro-valve, during which PDMS is spun and solidified on silicon wafer to achieve direct bonding of Silicon-PDMS film, this method is reversible bonding with low bonding strength. Another process is to build PDMS and SiO₂ mask layer, which is mainly valid in the production of biological chips, where oxygen plasma is used to treat PDMS and silicon substrates with oxide layer mask respectively and bond them together. This method is actually the bonding between PDMS and SiO₂ mask layer, but the bonding effect of SiO₂ film prepared by thermal oxidation method on silicon surface and PDMS is not realistic. However, during oxygen plasma surface treatment, PDMS can be successfully bonded with silicon wafers with passivation layer at room temperature and pressure. During the technology process of bonding modified PDMS with other substrate through oxygen plasma, it is generally believed that after oxygen plasma surface modification, PDMS substrates and cover sheets should be bonded immediately; otherwise, the surface of PDMS will quickly recover hydrophobicity, leading to bonding failure, so the operating process time is short, generally 1 ~ 10min. Usually, PDMS substrate and silicon substrate need to be bonded with corresponding fine structure, and it takes a certain time to align the structure pattern before bonding. Therefore, how to extend the duration of PDMS active surface becomes the key to ensure the bonding quality. After bonding mythology, the surface of PDMS treated by oxygen plasma has introduced hydrophilic -OH group and replaced the hydrophilic -CH group, so that the surface of PDMS shows extremely strong hydrophilicity. Similarly, due to the treatment of concentrated sulfuric acid on the silicon substrate, the surface contains a large number of Si-O bonds. In the process of oxygen plasma treatment, the Si-O bonds are broken, and a larger number of Si suspension bonds are formed on the surface. Thus, Si-OH bonds are formed by absorbing -OH in the air. When the treated PDMS is bonded to the silicon surface, the following reaction occurs between the Si-OH on the two surfaces. A strong new Si-O bond was formed between the silicon substrate and the PDMS, so as to complete the irreversible bonding between them.

3. Design

The WPT system design for smart contact lens can be divided into two main parts, one is the wireless power transfer unit antenna, and another one is the AC/DC converter. For the antenna part, spiral shape is applied for the circular characteristic as contact lens substrate, and for the circuitry part, both bridge rectifier and half-wave rectifier are tried to achieve best performance with lowest number of components. However, the challenge comes from its small size and the compatible power transfer efficiency.

3.1 Antenna Design

Firstly, for the size of antenna design, the dimension for contact lens is usually 14mm or 13mm diameter, thus, the dimension of the coil should be within this range. Meanwhile, the coil should be designed applicable for real case, which means all the components should not block the eye for normal eyesight. As for the light absorbing unit in eye structure, pupil, a small round hole in the centre of the iris in human eye, is the channel through which light enters the eye. Contraction of the upper iris pupillary sphincter causes the pupil to narrow, contraction of the pupil opening major causes the pupil to dilate, and dilation and contraction of the pupil control the amount of light entering the pupil. Since the dimension of pupil varies from 4mm to 8mm diameter within dark or light environments, the coil should be larger than the pupil dimension. In conclusion, the dimension for contact lens antenna should be with 10mm to 12mm diameter for safety and applicability considerations[13].

3.1.1 Leading Factor of Antenna Design

The most important parameter for antenna design in the first place is the S parameter, and for receiver side design, the main focus is S_{11} parameter, which describes the return loss, which is also known as reflected loss. It is the reflection of cable link due to impedance mismatch, and it is the reflection of a pair of lines themselves. The mismatch mainly occurs in the connector, but also may occur in the cable where the characteristic impedance changes, so the quality of construction is the key to improve the return loss[13]. Return losses introduce fluctuations in the signal and the returned signal is confused by the duplex gigabit network mistaking the received signal for the received one. Technically, return loss is the ratio of reflected wave power of transmission line port to incident wave power, expressed in absolute value in logarithmic form, generally positive, and is defined by Eq. 6:

$$R_L = -20\log|\Gamma| \text{ (dB)} \quad (6)$$

where Γ is the reflection index, the equation denotes that return loss is a parameter of signal reflection performance or indicates how many of the incident power is reflected back to the source. For example, suppose the return loss of the antenna is 10dB, then the reflected index is 0.316, which means when 10mW is being transferred, 70% of the power is absorbed by the antenna port. Generally, for implantable and wearable device, the return loss, which is the opposite number of S_{11} parameter, should be as close to 15dB as possible.

3.1.2 Design Method

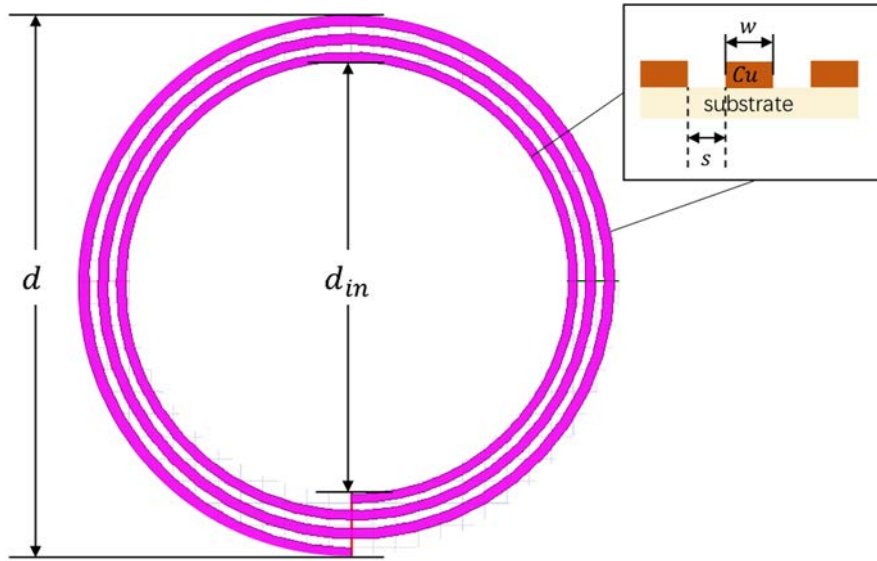


Figure 8. Circular Spiral Antenna.

For circular spiral antenna, the inductance of the antenna is the most important parameter which is mainly relied on the geometry design. As Figure 8 illustrates, the inductance relates to the circular spiral antenna line width w , fill-factor β , average turn diameter d_{avg} and copper magnetic permeability μ , shown as Eq. 7:

$$L_{spiral} = \frac{\mu N^2 d_{avg}}{2} \left(\ln \left(\frac{2.46}{\beta} \right) + 0.2\beta^2 \right), \quad (7)$$

where $\beta = \frac{d-d_{in}}{d+d_{in}}$, $d_{avg} = \frac{1}{2}(d + d_{in})$, $d = d_{in} + 2Nw + 2(N - 1)s$.

It predicts the inductance of antenna by the relationship of these geometry parameters. Based on the equation definition, a spiral antenna could be design using Archimedean spiral theory, denoted as Eq. 8:

$$r = r_0 + a\phi \quad (8)$$

Where r_0 is the starting radius, a is the growth rate of spiral, and ϕ denotes the angle or the arc value.

3.1.3 Receiver Antenna Design in HFSS

Circular Spiral antenna could be designed in HFSS by connecting functionalized curved based lines, and the function is defined as:

$$x(t) = r_0 e^{at} \cos(t),$$

$$\text{and } y(t) = r_0 e^{at} \sin(t).$$

which describes the spiral curve that related to the rotating time and initial inner circular radius. r_0 denotes the starting radius which is set to 4.8mm, and a is the increment of growth with the values of 10mm, the rotating end time is set to 6π to ensure the number of turns is 3. The line width of the antenna is set to 0.2mm for easy fabrication. Since in real condition, there are multiple layers inside human eyes, where there are different permeabilities affecting the performance of contact lens antenna. Thus, in simulation, an eye model is built to imitate the real condition for human eye as Figure 9.

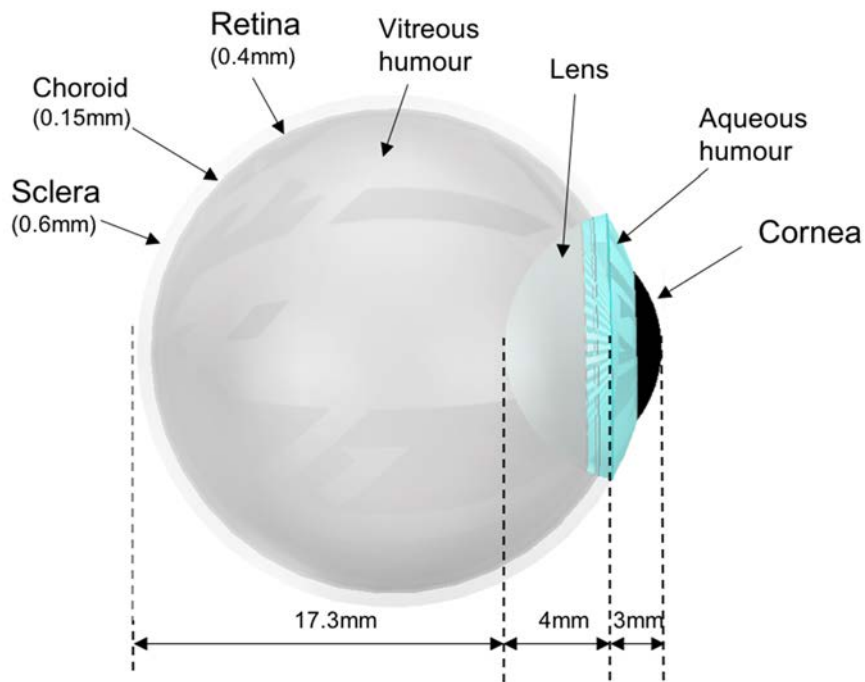


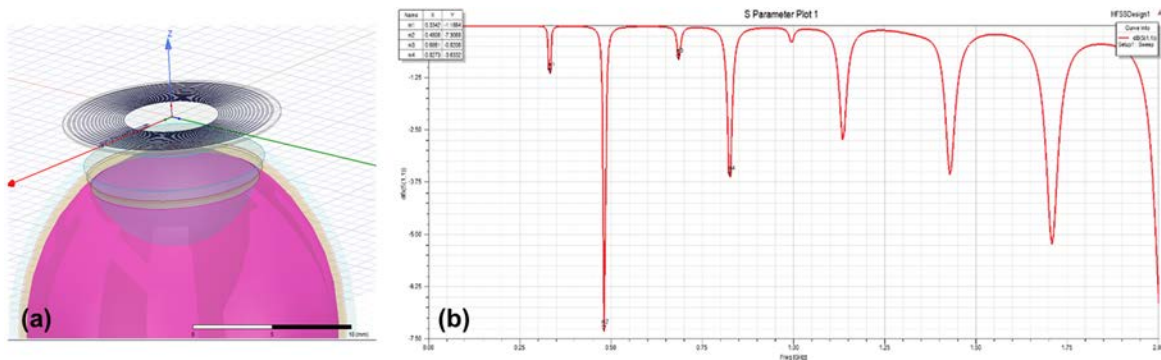
Figure 9.Eye model with dimension.

Adult eye sphere diameter is normally 24mm, with 3 outer layers Sclera, Choroid, and Retina. The lens is inside the eye sphere and just behind the cornea with aqueous humour liquid in between, however, it is formed as a nucleus shape with former convex curvature $R = 10mm$, posterior convex curvature $R = 6mm$, and front to rear diameter of 5mm. when building all those objects, their permeability, conductivity and density could be assigned for imitate the real case, as listed in Table 2.

Table 2. Electromagnetic parameters of eye tissues[15]

<i>Tissue</i>	<i>Relative permittivity ϵ_r</i>	<i>Electrical conductivity σ (S/m)</i>	<i>Density ρ(kg/m³)</i>
Aqueous Humour	72.7	2.220	994
Choroid	65.7	1.320	1050
Cornea	61.4	1.150	1062
Lens	38.4	0.353	1076
Retina	60.0	0.692	1036
Sclera	58.9	0.975	1032
Vitreous Humour	69.0	1.520	1005

These parameters are collected under 300MHz since the values do not change much under frequencies beyond this value, and also because the initial tuning frequency of the contact lens antenna is aimed around 300MHz. When the eyeball and the coil are built as Figure 10 (a), the S_{11} parameter was simulated as Figure 10 (b), as the simulated result shows, the first resonant frequency occurs at around 330MHz with a value of -1.15dB, which is not good either for frequency or S_{11} value. This best case is with inner radius 2.95mm, line width 0.05mm and with 16 turns of coil. But as the diagram of the construction shows, even if the coil is on top of the eyeball object, there is still an air gap in between to isolate them, which makes the situation similar as the coil simulation in the air. However, for the accurate simulation, the coil should touch the eyeball surface perfectly since all the electromagnetic parameters affect the inductance and capacitance of the coil design. once case with a PDMS surface wrapping on a transparent cylinder was tried to imitate the curved shape as Figure 11(a) shows, but the cylinder shape still makes the PDMS layer in touch with the air instead of the eyeball, thus the simulated outcome still in the range of 300MHz.

**Figure 10.** Flat geometry with simulation results (a) contact lens coil with eyeball (b) result of S_{11} .

Since the wrapping becomes an issue for the research progress, an eye cylinder was built to imitate the real case temporarily. However, same coil geometry is applied on different eye models, as the simulation result in Figure 11(c) indicates, the resonate frequency shifted

from 330MHz to 200MHz, and the S_{11} parameter decreases largely from -1.15dB to -10.4dB, which means more power or signal is absorbed by this receiver coil when the input signal and power for these two conditions are the same. Nevertheless, it also implies the significance of layer touches with each other during simulation and real case, that when the contact lens coil touches the surface of PMDS as well as the PDMS layer touches the eyeball surface, the result changes a lot. With the acknowledge about the importance of surface touching, the resonant frequency of the antenna is not tuned to frequency bands that verified by FDA, by adjusting the antenna geometry based on the relationship of wire length, wire gaps and the impedance, the tuned antenna can work on frequency band of 920MHz, which is applicable for implantable devices communications. This antenna dimension is with inner radius 5mm, outer radius 6mm, wire width 0.2mm and 3 coil turns.

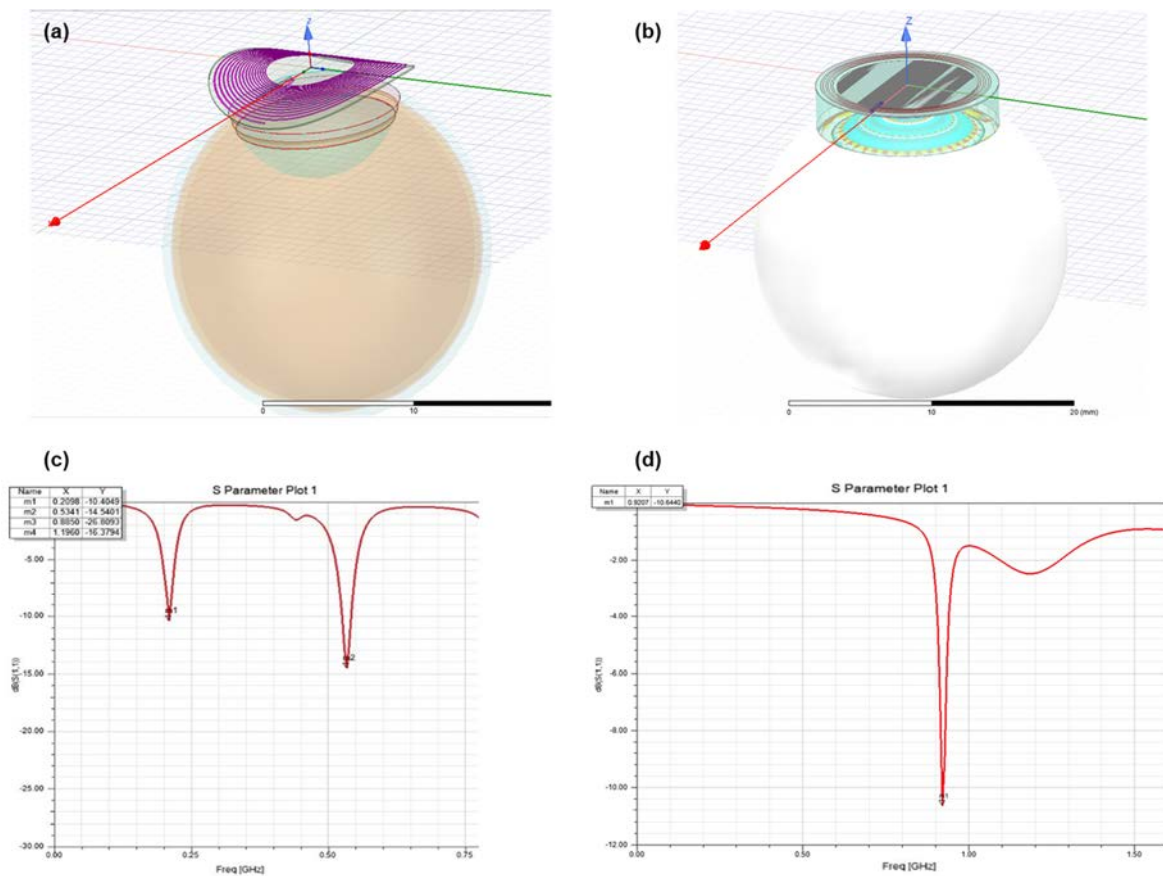


Figure 11. Bending geometry with simulation results: (a) coil wrapped on cylinder, (b) coil with eye cylinder and S_{11} of coil on eye cylinder (c) wrapped case (d) flat case.

Since the simulation outcome varies largely with the surface touching with each other, an accurate simulation should take the surface bonding into consideration. However, wrapping the circular PDMS layer onto the eyeball surface is not achievable by applying “wrap sheet” function in HFSS. Thus, an object with the outer surface shape of contact lens is created as

the PDMS layer to make the layer touches the eyeball, which is the substrate layer as the contact lens between the coil and the cornea. Although the commercialized contact lens we see from industrial fabrication turns to be a round hemispheroid since the commonly used material as contact lens is Polyhydroxyethylmethacrylate (HEMA) which earns good liquidity, in other words, when it contacts with the eyeball surface, it could automatically change shape to adhere with the cornea. Nevertheless, materials as HEMA with such high liquidity is hard to fabricate copper coil on top, instead, PDMS could be a good choice as the substrate for laboratorial used smart contact lens[16]. In terms of the actual shape contacting the eyeball, the surface of the eye sphere where the area is exactly as the commercialized contact lens size is detached as the PDMS shape, and a thickness of 100um is assigned as the substrate thickness, since it is the best way to imitate the form when it touches perfectly with the eyeball as Figure 12 (A) shows.

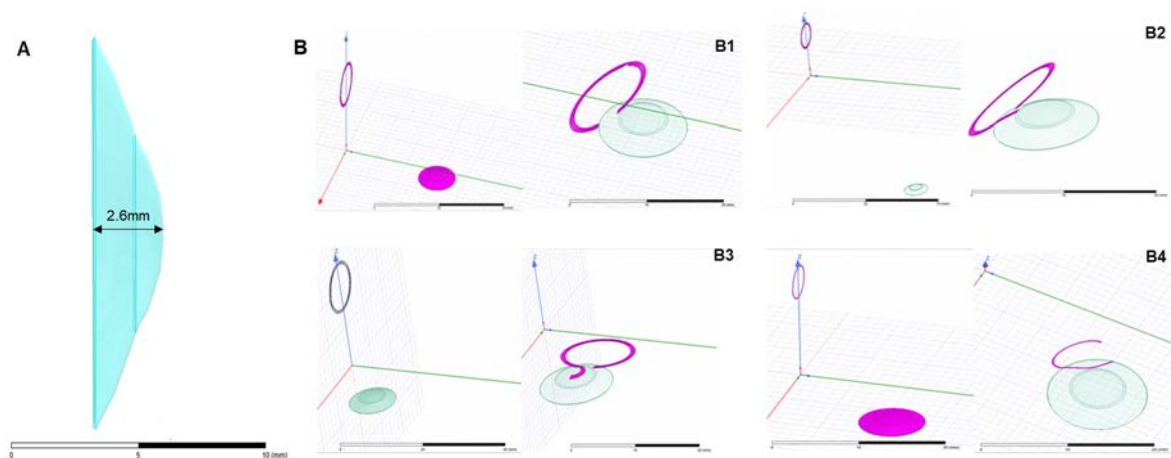


Figure 12. PDMS layer and warping attempts: (A) PDMS layer detached from eyeball and (B) Failed wrapping for different positions: (B1) Contact lens antenna position (0,0,20) PDMS position (0,30,0); (B2) Contact lens antenna position (0,0,20) PDMS position (0,50,-50); (B3) Contact lens antenna position (0,0,20) PDMS position (10,10,0); (B4) Contact lens antenna position (0,0,20) PDMS position (10,20,0).

However, when the substrate, coil and the eye model are built, the problem comes with wrapping the antenna onto the PDMS surface. For a normal sphere or a cylindrical object, it is easy to wrap a circular or rectangular sheet onto the surface, but for irregular shape object, wrapping function is not valid as the normal case.

Different positions for wrapping function is tested in HFSS, however, it seems irregular for wrapping with the object positions. Four examples are shown in Figure 12 (B), whether the PDMS layer is close to the coil or far away from the coil, they could not be wrapped perfectly, and the wrapping outcomes seem to be randomly distributed which indicates not

much clues to wrap the antenna onto the PDMS surface. By reading more papers and datasheets online, this problem is fixed by projecting sheet onto an object in HFSS using “project sheet” function, and the projected antenna and its minimum sized connection are shown as Figure 13.

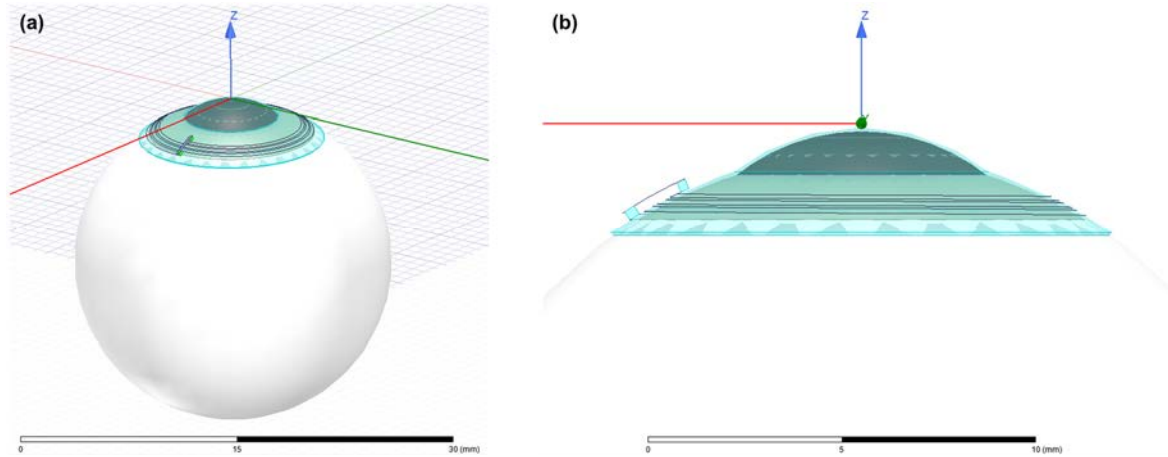


Figure 13. Projected antenna outcome: (a) projected contact lens antenna on eyeball and (b) the connection between two coil terminals.

With the same coil geometry for the 920MHz coil, the curved simulation appears a large frequency shift from 920MHz to 2.58GHz, which illustrates that the more accurate the simulation condition is, any small geometry or parameter differences would cause much more changes than one can expect. Since the result of same coil geometry differs a lot upon different shape of eyeball, the current density property is checked to investigate the reason of these two conditions, the result is as Figure 14.

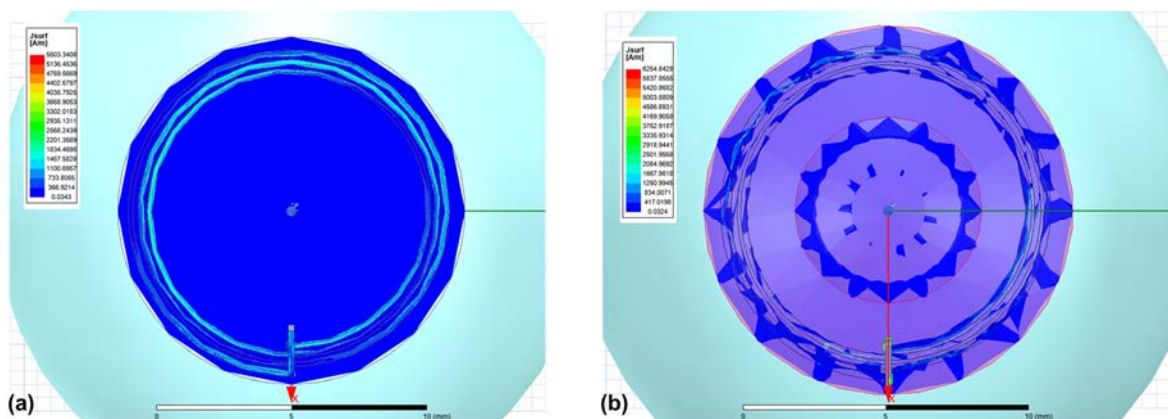


Figure 14. Current density of coil on (a) eye-cylinder and (b) eyeball model.

Although the measurement dimension standard of two diagram is slightly different, it is still obvious that the current concentration on eye-cylinder is much higher than the one on eyeball, where current is subtly generated, which indicates the electric field generated in

eyeball case is not strong which would not cause much power consumption, in other words, magnetic field generated around is not strong enough either that the resonate result is not idealistic.

For projected contact lens antenna, no matter how much the wire width, wire gap or increment differs, the resonant frequencies are all around 2GHz to 3GHz, thus, the expected verified tuning frequency should be 2.45GHz within 2.4GHz to 2.5GHz, under which the antenna could also transfer information back and forth using the WIFI frequency band. After multiple tries and parameter sweeping, both contact lens antenna either on eye cylinder or eyeball are tuned to around 2.45GHz.

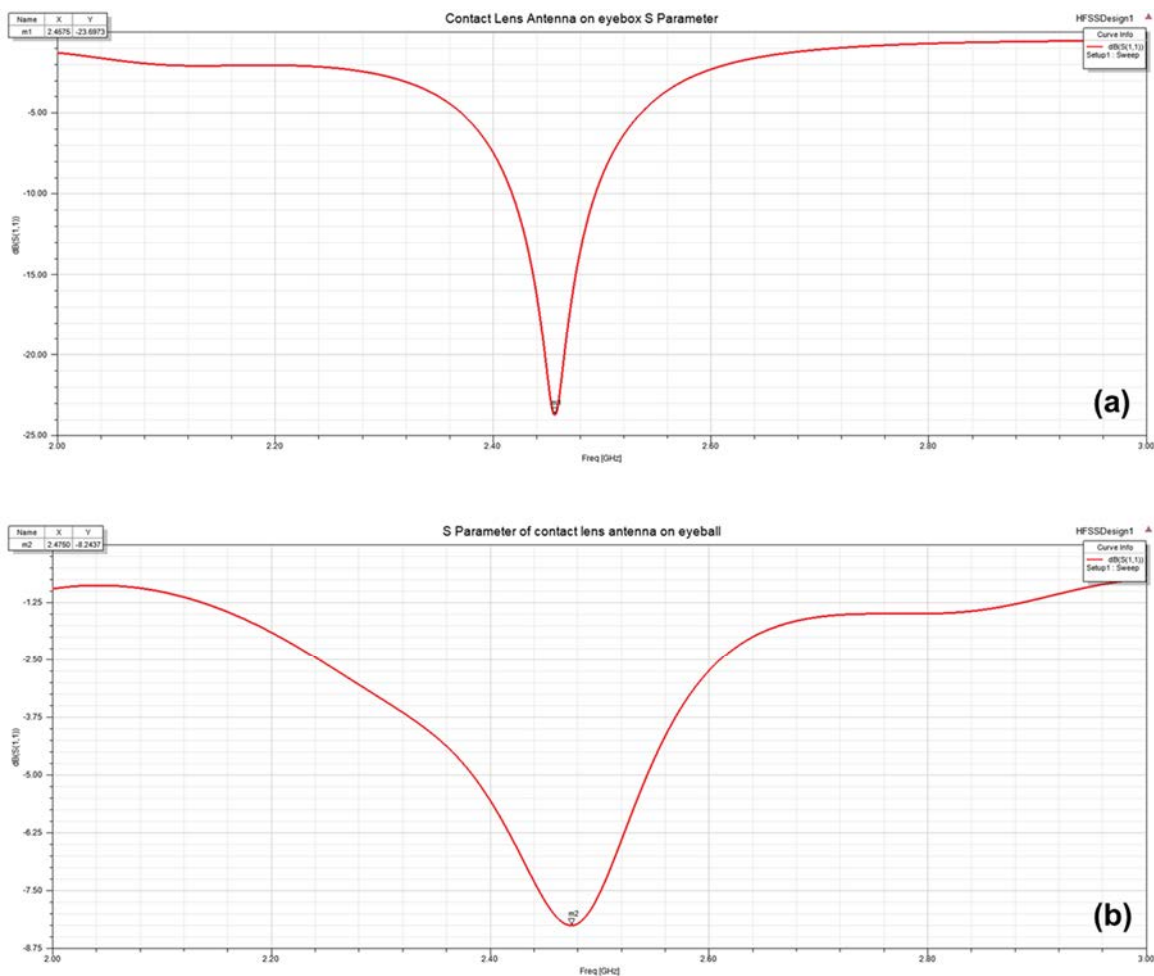


Figure 15. S_{11} simulation result of contact lens antenna on (a) flat eye-cylinder and (b) eyeball.

The Smith Chart is also a tool which implies the coupling and matching performance of antenna, which is a calculation diagram plotted on the reflection scatter plane with a family of equivalent circles of normalized input impedance or admittance. And it is also a diagram mainly for impedance matching of transmission lines. The Figure is composed of three

circles, which can be solved by graphical method in the problems of transmission lines and some waveguides to avoid complicated operations.

When the value is up above 0 axis, the antenna works as an inductor, when the value is below 0 axis, the antenna has more function as a capacitor. For points lying on the real axis line $x = 0$, and the impedance corresponding to each point on the real axis is pure resistance, which is called pure resistance line. The $|\Gamma| = 1$ circle, which is where $r = 0$, the corresponding impedance has pure reactance, called pure reactance circle. Thus, in Smith Chart, the perfectly tuned antenna should be as close to $r=1$ as possible.

As Figure 16 shows, (a) is the impedance of antenna on flat eye-cylinder, which resonates at 2.45GHz. As the graph indicates, the resonating frequency point is next to $r=1$ circle, and the impedance of this antenna is $0.8755 + 0.0159j$, where the resistance is quite low that would not affect the return loss. However, for Figure16(b), the Smith Chart circle is smaller than $r=1$, and the impedance of this antenna is $1.8541 + 0.7601j$, where the resistance is higher than the previous value, which would increase the power losses in transferring process. However, the imaginary part consists of the inductance and capacitance of the antenna design, it is not clear how much inductance and capacitance it gains, but based on the values, it can be predicted that all these two antennas work as inductance in the circuit since they have more inductively characteristic than capacitively one to make the imaginary part positive.

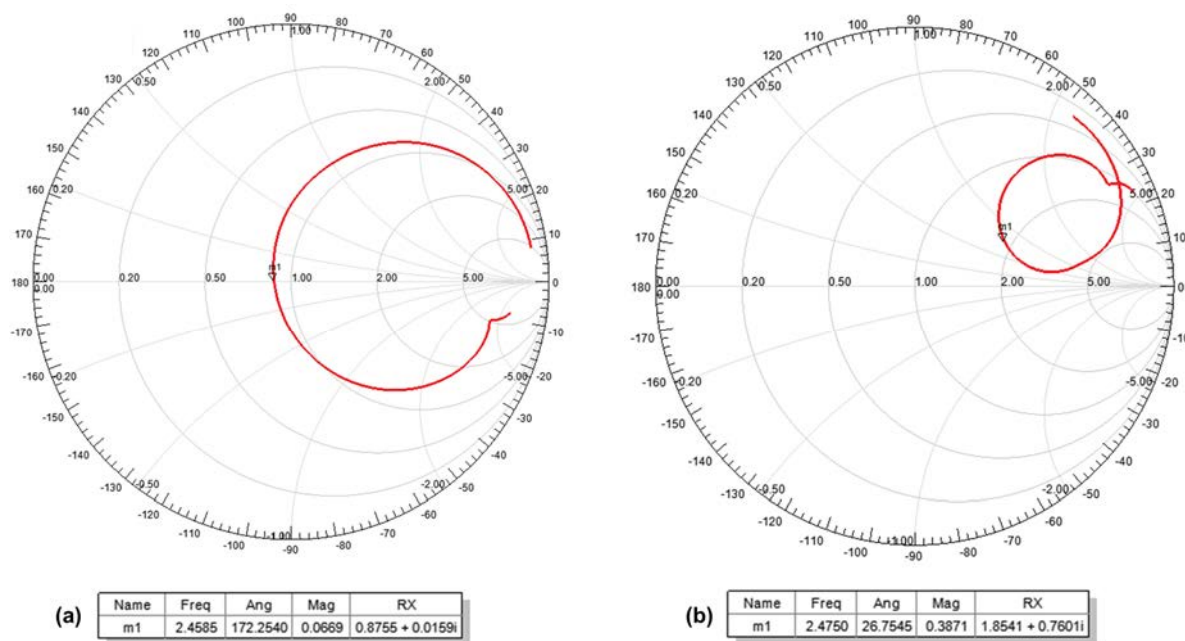


Figure 16. Smith Chart of contact lens antenna on (a) flat eye-cylinder and (b) eyeball.

3.1.4 Transmitter Antenna Design in HFSS

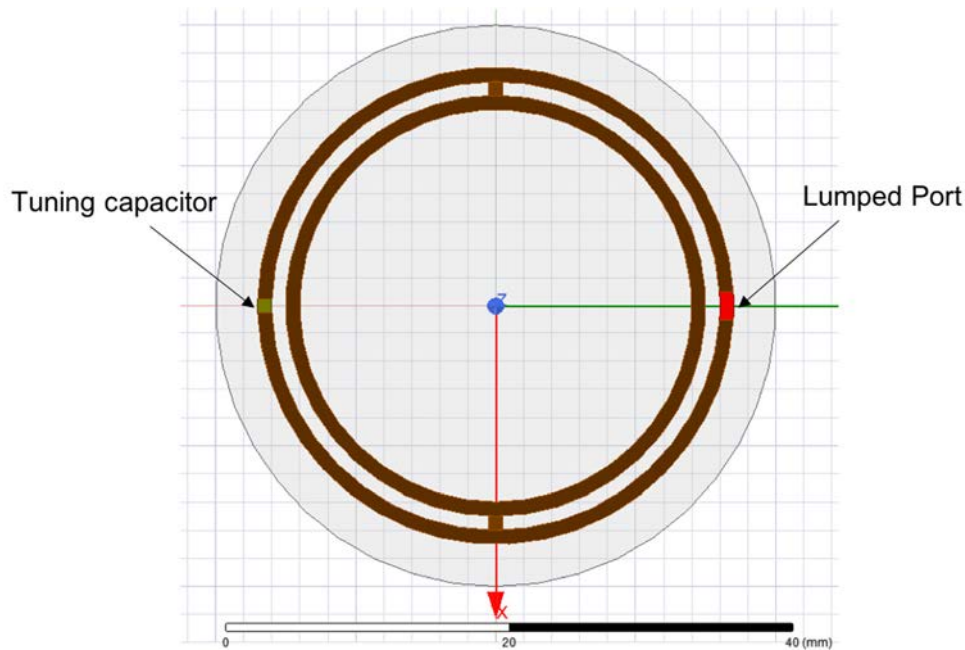


Figure 17. Transmitter antenna geometry

When the receiver side antenna has been designed, the transmitter one is also tried as the sizes of a piece of glass, since for contact lens, power transmitter unit could be loaded on normal glasses for safety and beauty. As Figure 17 shows, a glass with diameter 40mm is put at the bottom, and there are two concentric circles with wire width and wire gap both 1mm. The red rectangular on the right side is inserted as a lumped port for the excitation, the green one on the left is the tuning capacitor for matching the coil inductance. To make the system work and test the transferring performance during transmitter and receiver sides, the frequency of the transmitter antenna should be tuned to 2.45GHz as well. But due to the time limitation, this approach has not been finished now.

3.2 Circuit design

In the previous analysis, full-wave bridge rectifier is more efficient than half-wave rectifier without losing any signal. Thus, full-wave rectifier circuit was built as the AC/DC converter as Figure 18(a). However, for AD/DC converting the most vital issue is the power and current it transfers[17]. Based on the initially ideal for this project, the outcome of power transfer unit is to power an LED, which can work under normally 2-3 Volts, and the average current requirement is normally 30mA but the current only relates to the light intensity, which can be beyond the standard value.

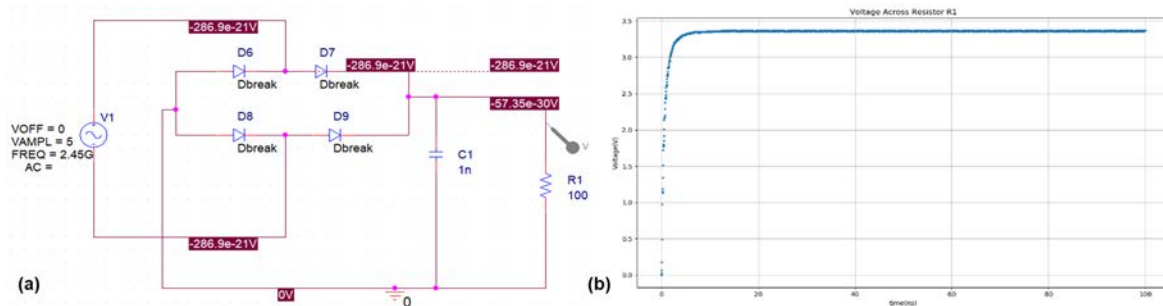


Figure 18. Full-wave rectifier: (a) circuit and (b) output voltage result.

As Figure 18(a) shows, the simulation result can be expected that when the sine wave is in positive region, D7 and D8 is working, when the wave is in negative half, D9 and D6 work with voltage drops. The smoothing capacitor C1 is added to take drop voltage of each cycle and also for deciding the rising time of the voltage, after which the circuit could be treated as a linear DC signal. As the simulation result shows in Figure 18(b), the voltage of the load resistor is around 3.3V.

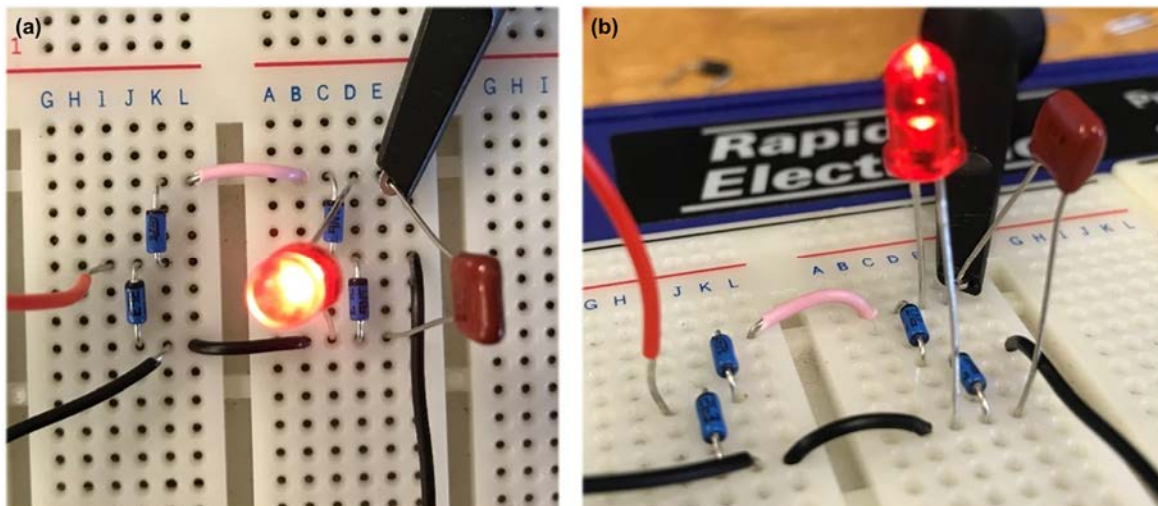


Figure 19. Full wave rectifier circuit construction on (a) top view (b) front view

After the simulated verifying, a basic circuit is built on bread board to test the feasibility as Figure 19. In the real case measurement, and LED is place instead of the resistor since the aim of this circuit is to power an LED, and it is easy to use LED to see the power transfer outcome clearly by light generation. In the testing circuit, 5Volts power is supposed to be transferred to the rectifier, thus the signal generator generates a sinusoidal wave with 5Volts amplitude and with 3MHz, since the highest frequency of normal generator is 1MHz, thus for the testing circuit, much lower frequency is applied, but it would not affect the voltage values of the circuit performance. The output voltage vs Input voltage result is shown as Figure 20.

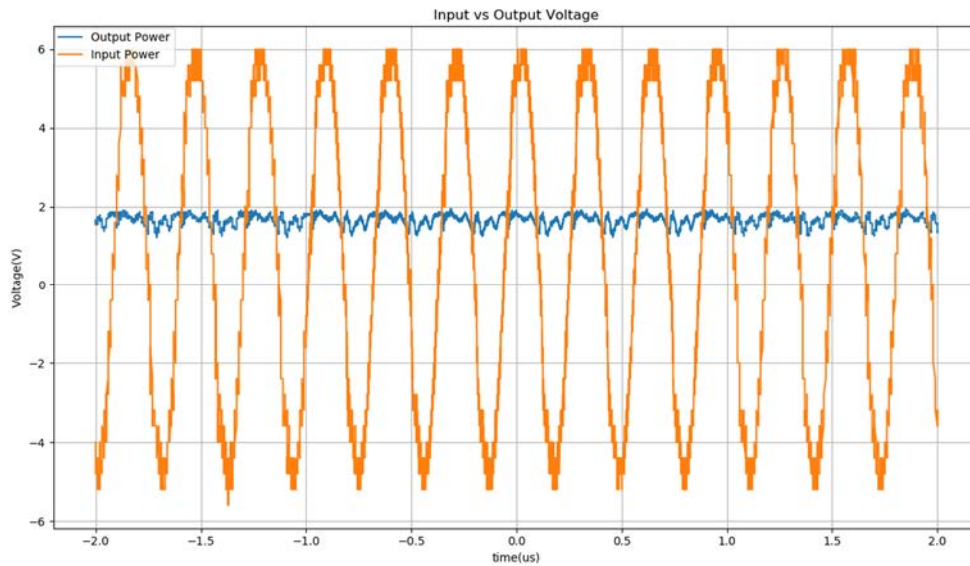


Figure 20. Output voltage vs Input voltage of testing circuit.

However, full-wave rectifier would occupy more space in the circuit, especially on the application of contact lens, where space is extremely limited. Thus, a half-wave rectifier is also built for less circuit components application.

As Figure 21 (a) indicates, the half-wave rectifier contains only three components, a diode, capacitor and a resistor. The voltage across the resistor is also tested as Figure 21 (b), since there is only one diode component which causes voltage drop, the output voltage increases to 4.3V, and because the frequency of simulation is such high at 2.45GHz, the charging and discharging process of smoothing capacitor is not obvious, thus the output voltage could be regarded as a stable DC output.

Half-wave circuit is also built for testing the performance, as is shown in Figure 22. The input signal is also 5V sinusoidal wave with frequency of 1MHz, the LED is also been powered by half-wave circuit, however, the light intensity is lower than full-wave circuit since the average voltage or power generation of half wave circuit is the half of the input signal since the other half is cut out.

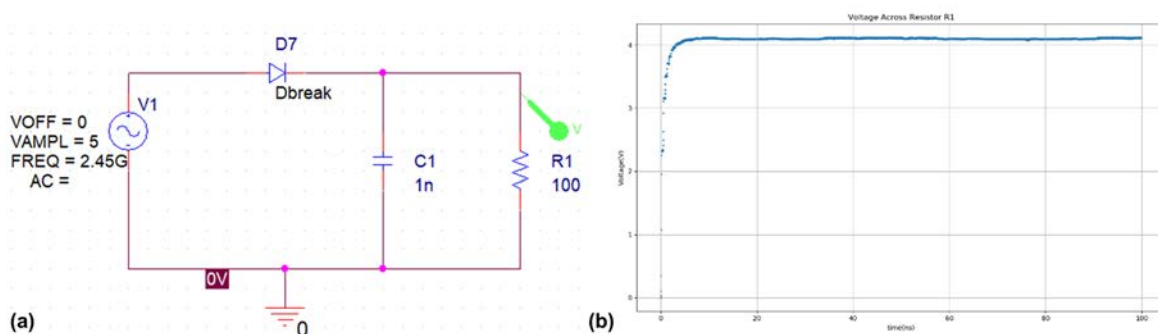


Figure 21.Half-wave rectifier: (a) circuit and (b) simulation.

This circuit test also indicates that even for 1MHz frequency, the signal is transferring or oscillating fast enough to be regarded as flat DC signals, but it is best to fabricate with rectifiers at least to avoid negative signal breaking the LED.

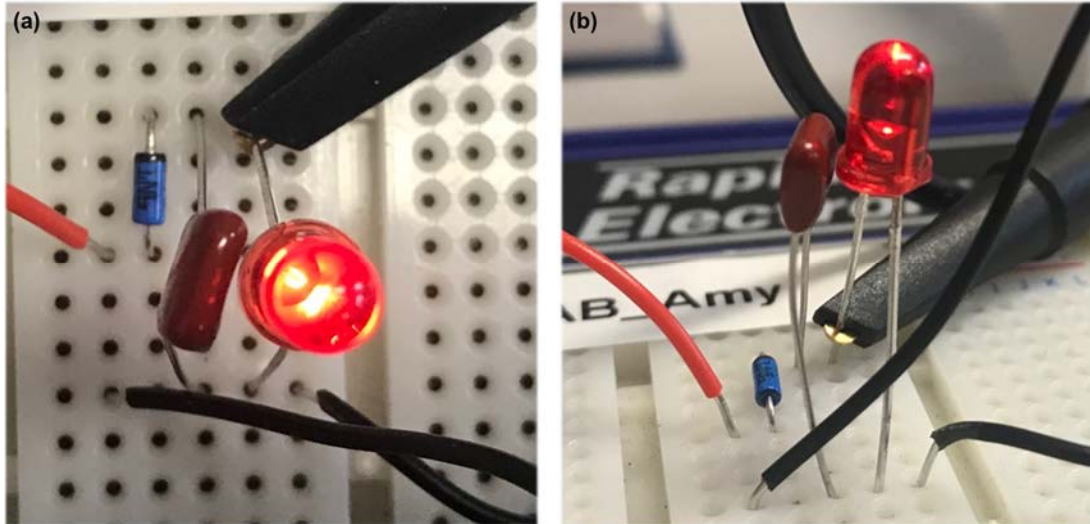


Figure 22.Half-wave rectifier circuit construction on (a) top view and (b) front view.

3.3 PCB design

The software Altium is used for the PCB layout design, and two versions were made for the same antenna with different circuit. Components in Figure 23(a) is placed with SOD323, 0805 and 0603 footprint encapsulation for diode, capacitor and LED separately, and the maximum size for the component is $2.4mm \times 1.25mm$. For the second version PCB, the shape of the substrate is changed to a round circle with diameter 13.4mm imitating the contact lens, and components are chosen to be smaller to concentrate together without blocking the pupil area. For this design, all components are encapsulated with 0201 footprint, which is the smallest dimension fabricating in commercialized market.

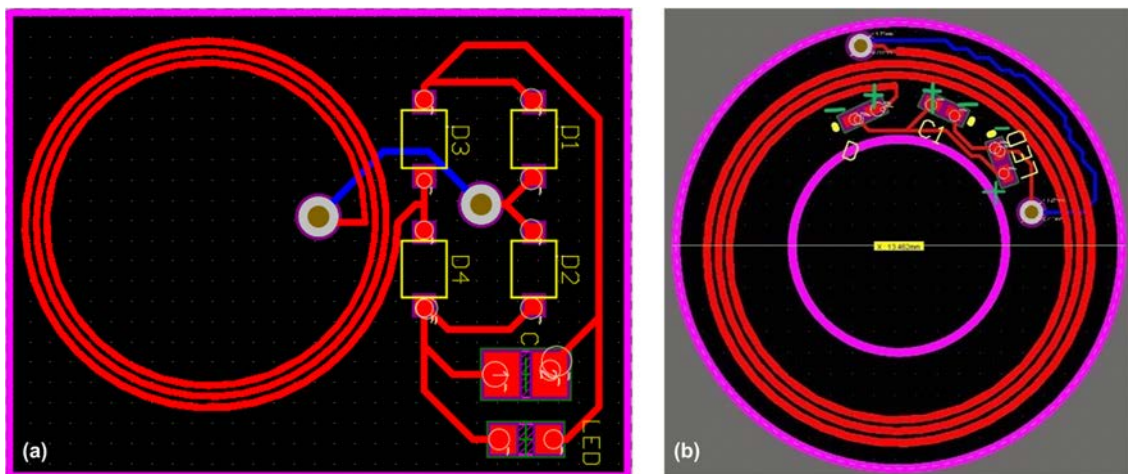


Figure 23.Two versions of PCB design with different component size and position.

4. Result

The first version of antenna is fabricated by technician in the school of engineering in University of Glasgow, however, the achievable technology for copper wire with fabricated on whether FR4 or flexible substrates is 0.2mm, but the antenna is designed with 0.1mm wire gap, this becomes a challenge for normal fabrication workshop. Thus, two versions are supposed to be fabricated, for the limited time duration, only the first version is fabricated by technicians in Rankin building, the second version is sent to a Chinese company to fabricate, and by the time of the author writing the report, that patch is still in the process of delivery.

4.1 Fabricated Antenna

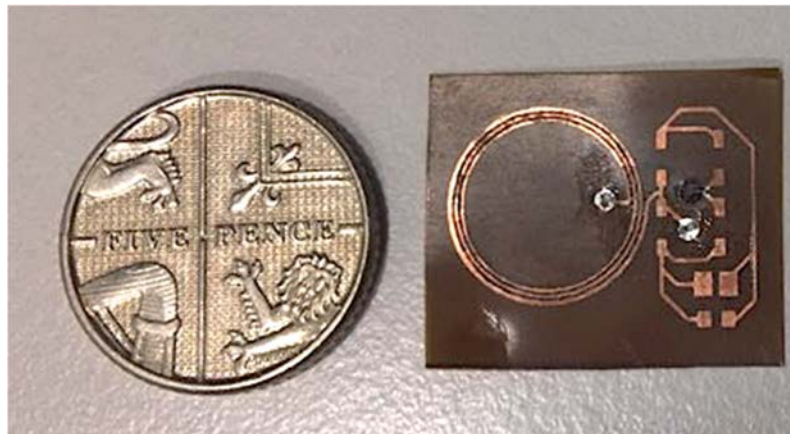


Figure 24. Fabricated antenna compared with a five pence size

As Figure 24 shows, the patch size is even smaller than one five pence coin. The antenna was tested under air, on hand tissue and on water surface that imitates the aqueous humour liquid in human eye. The testing process are shown as Figure 25, the frequency sweeping is from 10MHz to 20GHz, and the results are extracted from 10MHz to 3GHz since that is the frequency band for the usage of this contact lens antenna design. During the test of antenna performance, three samples are tested, and each condition for each antenna has three measurement values. It is shown in the result that, when the antenna is in the air, there is not much resonating points within 3GHz frequency, but when the contact lens antenna is put on hand, there are obvious resonating points from 900MHz to 1GHz, and for contact lens antenna on hand, the S_{11} performance is better than that on water surface. However, the resonate frequency of the contact lens antenna with extra circuit is not even similar as that in simulation, another condition is test with cut antenna without any circuit to imitate

the simulated antenna, but the resonate frequency of this version just shifted to around 1GHz, and the S_{11} parameter performance is similar as those with circuits.

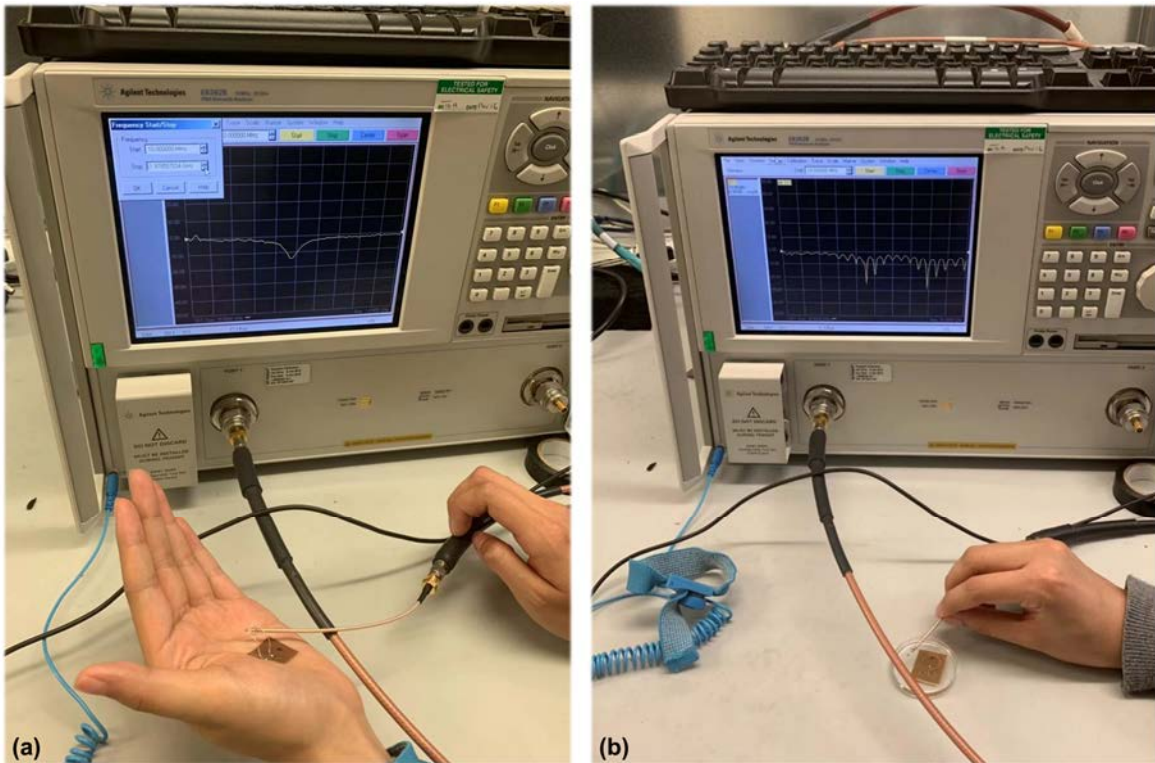
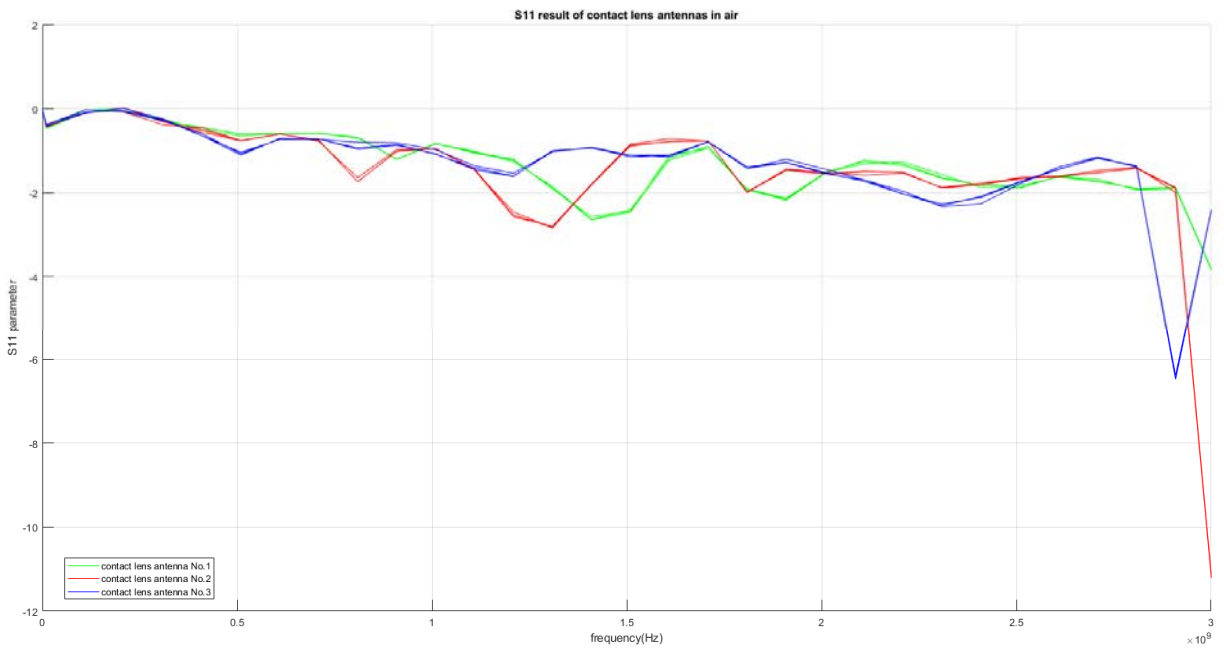
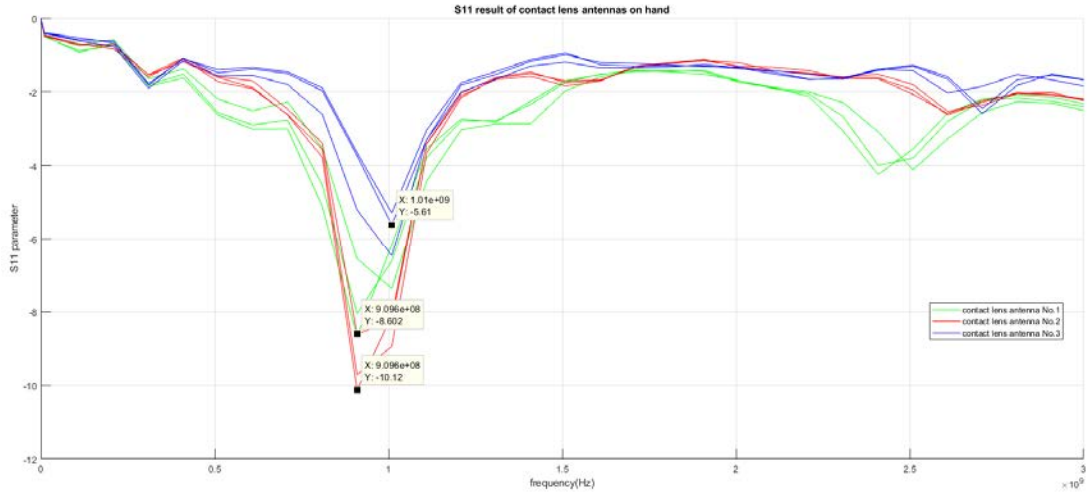


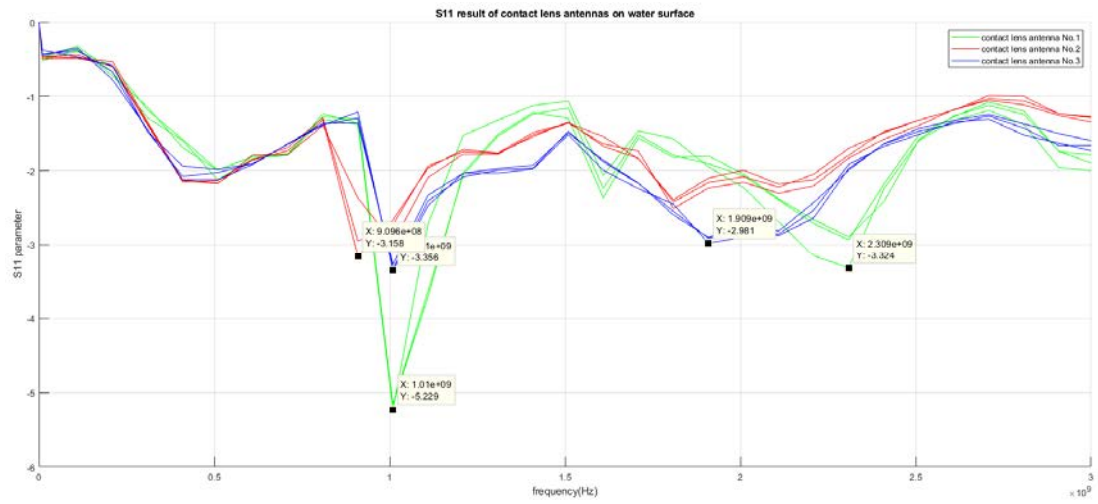
Figure 25. Antenna test under different conditions: (a) on hand and (b) on water surface.



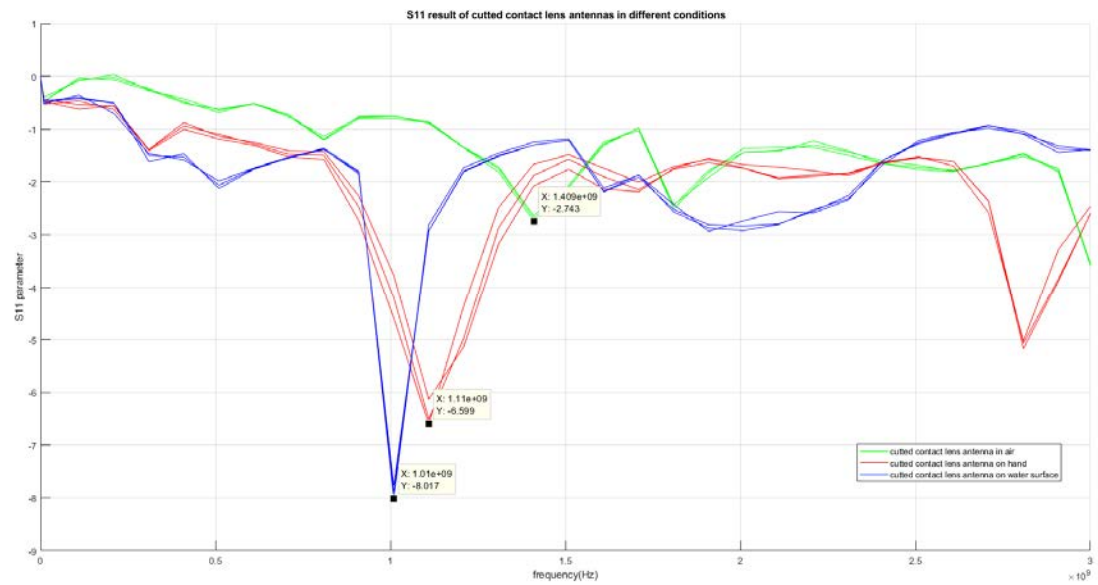
(a) S_{11} result of contact lens antenna in air



(b) S_{11} result of contact lens antenna on hand



(c) S_{11} result of contact lens antenna on water surface



(d) S_{11} result of cut contact lens antenna under different conditions

Figure 26. S_{11} parameter under different condition.

4.2 Laser Cutting

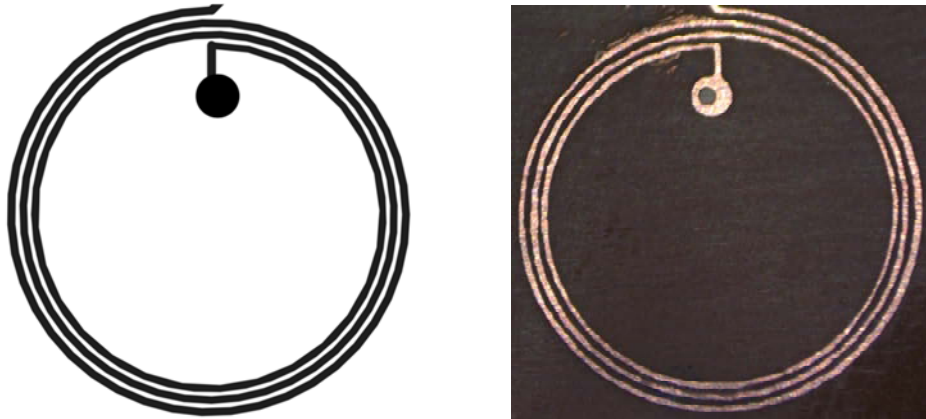


Figure 27. PCB compared with drawing graph.

Limited by the fabricating technology, the contact lens antenna fabricated in Rankine Building is not accurate as the design, which is clearer under microscope as Figure 27. Due to the fabrication limitation, it is clear that the fabricated antenna wire length is not equal enough, some area the line width is shorter and some place the line width is thicker, this may cause huge difference of the antenna resonating performance since the inductance and capacitance would change because of the uneven line width. Thus, the laser cutting method was tried to cut a mask for printing copper on top of that. As Figure 28(a) shows, since the PET substrate is too thick for cutting, the shape could not be cut through, additionally, since the antenna shape is a spiral curve rather than a circular form, for laser cutting method, all lines are divided into small rectangular segments, thus for spiral shape, the laser cutting pin oscillates a lot during cutting which makes the line more unstable. Nevertheless, for Polyimide cutting, the shape could be cut through since the layer is relatively thin, but it is hard to find the perfect power that could cut the lines without cutting through them. Thus, the second version of PCB is sent to a Chinese company to fabricate.

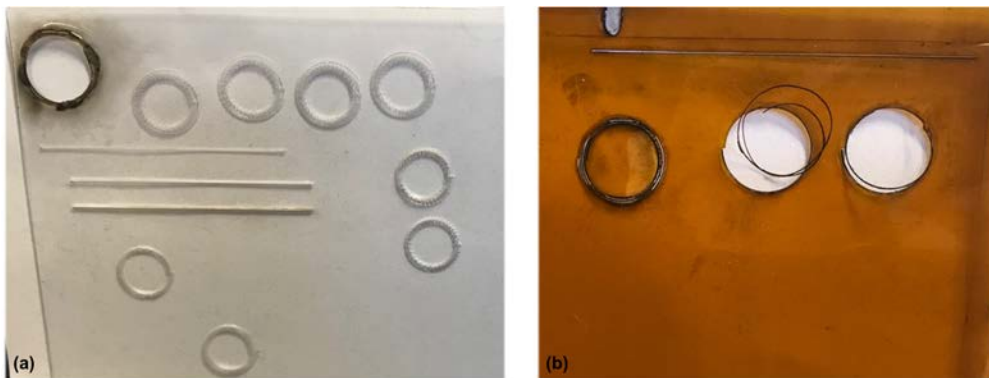


Figure 28. Laser cutting on different materials: (a) PET and (b) Polyimide.

5. Analysis and Discussion

The S_{11} result of the antenna differs a lot with the simulation, which may be caused by many issues. Such as the geometry effect and the condition effect. Since the line width of the fabricated antenna is thinner or even uneven than the designed geometry, which differs in the inductance and capacitance of the design. However, the results for different conditions also vary a lot since for different tissue or liquid environment, the permeability or conductivity is different, which would also cause errors.

5.1 Geometry Effect on Antenna

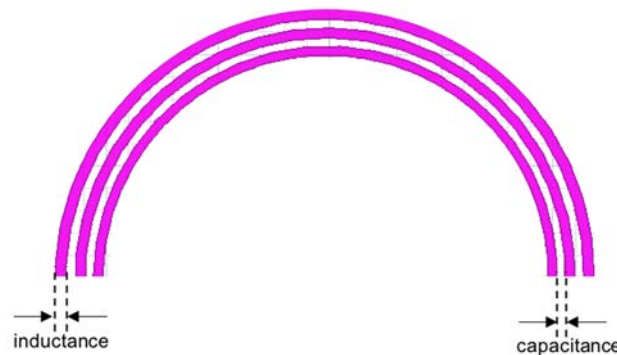


Figure 29. Antenna design geometry related to electrical parameters.

As Figure 29 shows, the width and length of the copper wire in antenna design is related to antenna inductance, and the gap between the two wires defines the capacitance of the coil, and based on the inductance and capacitance of the coil, the resonate frequency can be defined by Equation 2. For the fabricated antenna, the line width is not even, which may decrease the inductance of the designed antenna, and also increase the capacitance since the gap between two lines is wider. However, during the simulation procedure, circuit elements are not concluded, but for real fabrication, the circuit part as shown in Figure 30 increases more copper wires that enlarges the inductance of the wire, which decreases the resonating frequency. In future design, those tiny parts should also be concluded.

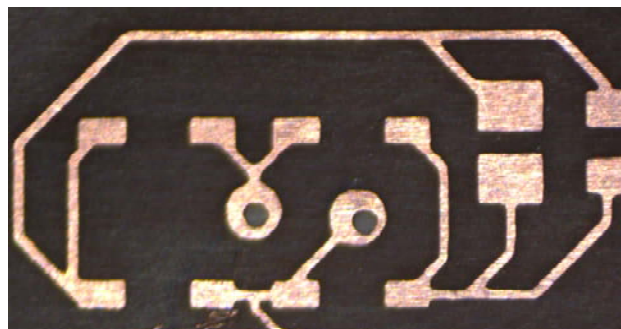


Figure 30. Circuit in PCB.

5.2 Different Conditions Effect on Antenna

As Table 2 listed, different tissues inside human body would generate various electrical parameters, and those parameters would change under sundry frequencies. However, this is because in the region radiated by the antenna, due to the change of the dielectric constant of the external space, the wavelength of the electromagnetic wave changes during the passage of the medium, which causes the resonant frequency of the antenna to change, and the performance is deviated at the actual used frequency shown as Eq.9:

$$\lambda = \frac{c}{f*\sqrt{\epsilon_r}} \quad (9)$$

As above equation illustrates, the When the frequency of operation is constant, the wavelength of the antenna is related to the dielectric constant. For different sections in eye model, the dielectric constant varies to make the resonating frequency, but in the real testing environment, the dielectric values of hand tissue and water is different from that as the eye sections, which causes the diversities of the measurement.

The parameters of the dielectric substrate be considered when designing the antenna are mainly thickness, dielectric constant, and tangent loss angle. The dielectric constant of most PCB materials varies with frequency as well, taking hard PCB board as an example, the typical dielectric constant of FR4 is 4.2-4.4 at DC current and 3.9 at 2GHz, which decreases with increasing frequency. Thus, as the frequency increased, the corresponding material thickness needs to be increased. For instance, at 900MHz frequency, the PCB thickness (1.6mm) is 5% of the electrical length and 15% at 11GHz. Therefore, the dielectric constant of glass fibre has an increasing influence on the electrical length. As for the dielectric constant problem, the speed at which an electrical signal propagates is inversely proportional to the square root of the dielectric constant. The lower the dielectric constant, the faster the signal transmission speed, although high dielectric constant can reduce field leakage and cross-coupling effect. The commonly used PCB dielectric is FR4 material, and the relative air dielectric constant is 4.2-4.7. This dielectric constant varies with temperature and can vary up to 20% over a temperature range of 0-70 degrees, in other words, the change in dielectric constant will cause a 10% change in line delay. The higher the temperature, the greater the delay. And the resonate frequency is related to the loss of the medium, where the tangent angle loss is 0.025 for general FR-4 at 1MHz.

6. Conclusions and Further Work

6.1 Conclusions

The project goal is to design a wireless power transfer unit to power an LED as a load. During this process, HFSS software is used as the simulation of contact lens antenna, and Altium is used for the PCB design. The final version of the antenna is designed within diameter of 12mm, line width 0.2mm and with only 3 turns of coil. The inner diameter of the antenna is 10mm which exactly avoid blocking the light absorbing unit pupil in human eye. In addition, the designed resonate frequency is 2.45GHz which can transfer energy in long distance and communication with WIFI signal simultaneously. However, due to the fabrication technology limit and time shortage, only one version is made but with less perfect performance, the frequency tested on hand shifted to 900MHz from the designed value 2.45GHz. Since the testing conditions are different as the simulated environment, which causes the diversities of dielectric constant of various tissue sections, thus, affecting the resonant performance of contact lens antenna.

6.2 Suggestions for Further Work

In terms of the further improvement, there are two main aspects that may contributes to the integrity.

6.2.1 Antenna Improvement

The second version antenna is fabricated by a Chinese company, and the graph is as follows:



Figure 31. Second-version antenna.

For implantable devices, the implanted section should be flexible and stretchable enough since inside human body, the position and construction would change, which may cause the differences of the coil gaps and width. Thus, the antenna shape could change to serpentine antenna as Figure 31 shows, which is highly stretchable [18].[18]

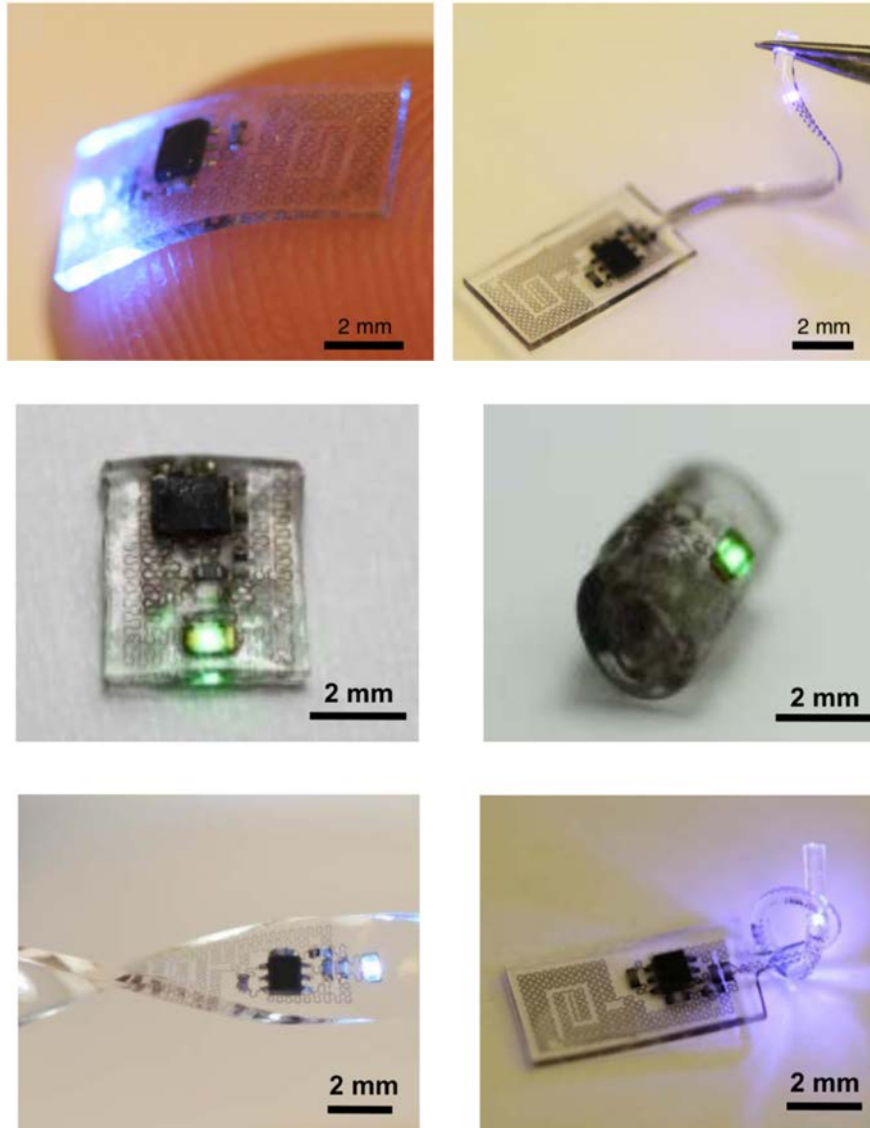


Figure 32. Serpentine antenna.

6.2.2 Fabrication Improvement

The designed line width for this spiral antenna is 0.2mm and the wire gap is 0.1mm, although this dimension is beyond PCB fabrication technology, it is still large for nano fabrication. In the future, antenna sizes at this range would go for nano fabrication to make the mask or the later encapsulation with PDMS or PMMA materials.

Reference

- [1]. Health Jade. (2019). *Pacemaker - Heart Pacemaker Indications, How a Pacemaker Work*. [online] Available at: <https://healthjade.net/pacemaker/>
- [2]. Katz, D. and Akiyama, T. (2007). Pacemaker Longevity: *The World's Longest-Lasting VVI Pacemaker*. *Annals of Noninvasive Electrocardiology*, 12(3), pp.223-226.
- [3]. En.wikipedia.org. (2019). *Cochlear implant*. [online] Available at: https://en.wikipedia.org/wiki/Cochlear_implant
- [4]. IEEE Spectrum: *Technology, Engineering, and Science News*. (2019). Full Page Reload. [online] Available at: <https://spectrum.ieee.org/tech-talk/biomedical/devices/google-working-on-smart-contact-lens-to-monitor-diabetes>
- [5]. Nytimes.com. (2019). *Novartis Joins With Google to Develop Contact Lens That Monitors Blood Sugar*. [online] Available at: <https://www.nytimes.com/2014/07/16/business/international/novartis-joins-with-google-to-develop-contact-lens-to-monitor-blood-sugar.html>
- [6]. Park, J., Kim, J., Kim, S., Cheong, W., Jang, J., Park, Y., Na, K., Kim, Y., Heo, J., Lee, C., Lee, J., Bien, F. and Park, J. (2018). Soft, smart contact lenses with integrations of wireless circuits, glucose sensors, and displays. *Science Advances*, 4(1), p.eaap9841.
- [7]. Hannan, M., Mutashar, S., Samad, S. and Hussain, A. (2014). Energy harvesting for the implantable biomedical devices: issues and challenges. *BioMedical Engineering OnLine*, 13(1), p.79.
- [8]. Narayanamoorthi, R. (2019). Modeling of Capacitive Resonant Wireless Power and Data Transfer to Deep Biomedical Implants. *IEEE Transactions on Components, Packaging and Manufacturing Technology*, 9(7), pp.1253-1263.
- [9]. U.-M. Jow and M. Ghovanloo, "Design and optimization of printed spiral coils for efficient transcutaneous inductive power transmission," *IEEE Transactions on biomedical circuits and systems*, vol. 1, no. 3, pp. 193-202, 2007.
- [10]. M. Schormans, V. Valente, and A. Demosthenous, "Practical Inductive Link Design for Biomedical Wireless Power Transfer: A Tutorial," *IEEE Transactions on Biomedical Circuits and Systems*, vol. 12, no. 5, pp. 1112-1130, July 2018.
- [11]. Z. Yang, W. Liu, and E. Basham, "Inductor Modeling in Wireless Links for Implantable Electronics," *IEEE Transactions on Magnetics*, vol. 43, no. 10, pp. 3851-3860, Oct. 2007.
- [12]. En.wikipedia.org. (2019). *ITU Region*. [online] Available at: https://en.wikipedia.org/wiki/ITU_Region
- [13]. Chiou, J., Hsu, S., Liao, Y., Huang, Y., Yeh, G., Kuei, C. and Dai, K. (2016). Toward a Wirelessly Powered On-Lens Intraocular Pressure Monitoring System. *IEEE Journal of Biomedical and Health Informatics*, 20(5), pp.1216-1224.
- [14]. Lingley, A., Ali, M., Liao, Y., Mirjalili, R., Klonner, M., Sopenan, M., Suihkonen, S., Shen, T., Otis, B., Lipsanen, H. and Parviz, B. (2011). A single-pixel wireless contact lens display. *Journal of Micromechanics and Microengineering*, 21(12), p.125014.
- [15]. Itis.swiss. (2019). *Tissue Frequency Chart » IT'IS Foundation*. [online] Available at: <https://itis.swiss/virtual-population/tissue-properties/database/tissue-frequency-chart/>
- [16]. Yin, R., Xu, Z., Mei, M., Chen, Z., Wang, K., Liu, Y., Tang, T., Priyadarshi, M., Meng, X., Zhao, S., Deng, B., Peng, H., Liu, Z. and Duan, X. (2018). Soft transparent graphene contact lens electrodes for conformal full-cornea recording of electroretinogram. *Nature Communications*, 9(1).
- [17]. Gutruf, P., Krishnamurthi, V., Vázquez-Guardado, A., Xie, Z., Banks, A., Su, C., Xu, Y., Haney, C., Waters, E., Kandela, I., Krishnan, S., Ray, T., Leshock, J., Huang, Y., Chanda, D. and Rogers, J. (2018). Fully implantable optoelectronic systems for battery-free, multimodal operation in neuroscience research. *Nature Electronics*, 1(12), pp.652-660.
- [18]. Park, S., Brenner, D., Shin, G., Morgan, C., Copits, B., Chung, H., Pullen, M., Noh, K., Davidson, S., Oh, S., Yoon, J., Jang, K., Samineni, V., Norman, M., Grajales-Reyes, J., Vogt, S., Sundaram, S., Wilson, K., Ha, J., Xu, R., Pan, T., Kim, T., Huang, Y., Montana, M., Golden, J., Bruchas, M., Gereau, R. and Rogers, J. (2015). Soft, stretchable, fully implantable miniaturized optoelectronic systems for wireless optogenetics. *Nature Biotechnology*, 33(12), pp.1280-1286.